

### **Point-by-point reply to co-editor request for minor corrections**

**Paper: Spatial, temporal and source contribution assessments of BC over the northern interior of South Africa (acp-2016-934)**

We thank the co-editor for accepting the paper, with minor corrections. Below is a point-by-point reply (in blue font) to the comments of the co-editor (in black font).

**It is my pleasure to accept your revised manuscript for publication in ACP. I only request correction of a few minor issues listed below. Thank you for considering the detailed referees' comments carefully.**

The authors thank the co-editor for the positive remarks. All the issues were addressed, as indicated below.

**1) Please complete the reference Sehloho et al. 2017 by adding the university etc.**

The reference were completed and now reads "Sehloho, R.M.: An assessment of atmospheric organic and black carbon at Welgegund. PhD thesis in preparation, North-West University, Potchefstroom Campus, South Africa, 2017."

**2) Check font sizes of all Figures for proper size when printed. They seem to be very small now, particularly for the complex multi-panel figures.**

The marked-up version of the paper that was re-submitted only contains the new figures and not the previous (old) figures, since this duplication made the paper very messy.

Two improvements were made on all figures:

- The text on all figures were increased by 1 to 4 text size units, as allowed without making the figures too crowded.
- All figures were inserted as full page width figures in the updated paper, instead of shrinking the figures to the estimated size in which they will be printed. This will allow the publishers to shirk the figures as they see fit and allow maximum image quality.

**I will finally accept after a quick check of the revised figures.**

The authors thank the co-editor for the professional manner in which the review process was handled.

# Spatial, temporal and source contribution assessments of black carbon over the northern interior of South Africa

Kgaugelo Euphinia Chiloane<sup>1</sup>, Johan Paul Beukes<sup>1</sup>, Pieter Gideon van Zyl<sup>1</sup>, Petra Maritz<sup>1</sup>, Ville Vakkari<sup>2</sup>, Miroslav Josipovic<sup>1</sup>, Andrew Derick Venter<sup>1</sup>, Kerneels Jaars<sup>1</sup>, Petri Tiitta<sup>1,3</sup>, Markku Kulmala<sup>4</sup>, Alfred Wiedensohler<sup>5</sup>, Catherine Liousse<sup>6</sup>, Gabisile Vuyisile Mkhathshwa<sup>7</sup>, Avishkar Ramandh<sup>8</sup>, Lauri Laakso<sup>1,2</sup>

[1] {Unit for Environmental Sciences and Management, North-West University, Potchefstroom Campus, South Africa}

[2] {Finnish Meteorological Institute, Helsinki, Finland}

[3] {Department of Environmental and Biological Sciences, Univ. of Eastern Finland, P.O. Box 1627, 70211 Kuopio, Finland}

[4] {Department of Physics, University of Helsinki, Finland}

[5] {Leibniz Institute for Tropospheric Research, Leipzig, Germany}

[6] {Laboratoire d'Aérodologie, Université Paul Sabatier-CNRS, OMP, 14 Avenue Edouard Belin, 31400 Toulouse, France}

[7] {Research, Testing and Development, Eskom SOC Ltd, Rosherville, South Africa}

[8] {Sasol Technology R&D (Pty) Limited, South Africa}

Correspondence to: J.P. Beukes (paul.beukes@nwu.ac.za)

## Abstract

After carbon dioxide (CO<sub>2</sub>), aerosol black carbon (BC) is considered to be the second most important contributor to global warming. This paper presents equivalent black carbon (eBC) (derived from an optical absorption method) data collected from three sites in the interior of South Africa, where continuous measurements were conducted, i.e. Elandsfontein, Welgedund and Marikana, as well elemental carbon (EC) (determined by evolved carbon method) at five

1 sites where samples were collected once a month on a filter and analysed off-line, i.e. Louis  
2 Trichardt, Skukuza, Vaal Triangle, Amersfoort and Botsalano.

3 Analyses of eBC and EC spatial mass concentration patterns across the eight sites indicate that  
4 the mass concentrations in the South African interior are in general higher than what has been  
5 reported for the developed world and that different sources are likely to influence different sites.  
6 The mean eBC or EC mass concentrations for the background sites (Welgegund, Louis  
7 Trichardt, Skukuza, Botsalano) and sites influenced by industrial activities and/or nearby  
8 settlements (Elandsfontein, Marikana, Vaal Triangle and Amersfoort) ranged between 0.7 and  
9 1.1, and 1.3 and 1.4  $\mu\text{g}/\text{m}^3$ , respectively.

10 Similar seasonal patterns were observed at all three sites where continuous measurement data  
11 were collected (Elandsfontein, Marikana and Welgegund), with the highest eBC mass  
12 concentrations measured during June to October, indicating contributions from household  
13 combustion in the cold winter months (June-August), as well as savannah and grassland fires  
14 during the dry season (May to mid-October). Diurnal patterns of eBC at Elandsfontein,  
15 Marikana and Welgegund indicated maximum concentrations in the early mornings and late  
16 evenings, and minima during daytime. From the patterns it could be deduced that for Marikana  
17 and Welgegund, household combustion, and savannah and grassland fires were the most  
18 significant sources, respectively.

19 Possible contributing sources were explored in greater detail for Elandsfontein, with five main  
20 sources being identified as coal-fired power stations, pyrometallurgical smelters, traffic,  
21 household combustion, as well as savannah and grassland fires. Industries on the Mpumalanga  
22 Highveld are often blamed for all forms of pollution, due to the  $\text{NO}_2$  hotspot over this area that  
23 is attributed to  $\text{NO}_x$  emissions from industries and vehicle emissions from the Johannesburg-  
24 Pretoria megacity. However, a comparison of source strengths indicated that household  
25 combustion, and savannah and grassland fires were the most significant sources of eBC,  
26 particularly during winter and spring months, while coal-fired power stations, pyro-  
27 metallurgical smelters and traffic contribute to eBC mass concentration levels year round.

# 1 Introduction

Aerosol black carbon (BC) is the carbonaceous fraction of ambient particulate matter that absorbs incoming short-wave solar radiation and terrestrial long-wave radiation, which has a warming effect on the atmosphere (IPCC, 2013). Although BC has a relatively short atmospheric lifetime (days to weeks), it has significant regional effects on temperature, cloud amount and precipitation. Over snow-covered areas, the surface albedo can be significantly reduced due to the deposition of BC, and this may considerably influence the local and regional climate (Ramanathan and Carmichael, 2008; Jacobson, 2004). Direct observations of reduced albedo resulting from long-range-transported BC into Arctic areas were reported by Stohl et al. (2006). It was estimated that BC may have contributed to more than half of the observed Arctic warming since 1890, most of this occurring during the last three decades (Shindell and Faluvegi, 2008). After CO<sub>2</sub>, BC is considered to be the second most important contributor to global warming (Bond et al., 2004; IPCC, 2013). According to some authors, reducing BC emissions may be the fastest means of slowing global warming in the near future. In addition to the afore-mentioned effects, BC is a major contributor to fine particulate matter in the atmosphere that can also have negative health effects (Hansen et al., 1984, Cachier, 1995; IPCC, 2013).

Atmospheric BC is a primary species (Putaud et al., 2004; Pöschl, 2005) that is emitted by combustion processes, particularly from fossil fuel combustion, diesel engine exhaust, as well as open biomass fires and household combustion (Cachier, 1995; Cooke and Wilson, 1996; Bond and Sun, 2004; IPCC, 2013). Globally, approximately 20% of BC is emitted from residential biofuel burning, 40% from fossil fuels and 40% from open biomass burning such as forest and savannah fires (Hansen et al., 1988; Cooke and Wilson, 1996; Wolf and Cachier, 1998; Pope, 2002;). BC from fossil fuels is estimated to contribute a global mean radiative forcing of 0.04 watts per square metre (W/m<sup>2</sup>) (IPCC, 2013).

There are large uncertainties associated with emissions of BC, its aging during atmospheric transportation and its removal by precipitation (Bond and Sun, 2004), which are reflected in uncertainties in the global effect of BC (e.g. Bond et al., 2013). Presently, the majority of aerosol radiative impact assessments are based on models (Bond et al., 2013; IPCC, 2013), both on local and global scales, which incorporate measured aerosol properties. However, this approach involves several assumptions (e.g. assuming aerosol properties and the use of global instead of regional emission inventories for under sampled/characterised regions). Considering

1 the relatively short atmospheric lifetime of BC, such assumptions could lead to significant  
2 uncertainties, especially on regional scales (Andreae and Gelencser, 2006; Masiello, 2004;  
3 Bond et al., 2013; Kuik et al., 2015). For a better understanding of the transport, removal and  
4 climatic impacts of atmospheric BC, accurate and up-to-date measurements covering large  
5 spatial areas and long temporal periods are required.

6 Africa is one of the least studied continents, although it is regarded as the largest source region  
7 of atmospheric BC (Liousse et al., 1996; Kanakidou et al., 2005). Southern Africa is an  
8 important sub-source region, with savannah and grassland fires (anthropogenic and natural)  
9 being prevalent across this region, particularly during the dry season, when almost no  
10 precipitation occurs (Formenti et al., 2003; Tummon et al., 2010; Laakso et al., 2012; Vakkari  
11 et al., 2014; Mafusire et al., 2016). Studies by Swap et al. (2004) indicated that savannah and  
12 grassland fire plumes from southern Africa affect Australia and South America. South Africa  
13 is the economic and industrial hub of southern Africa with large anthropogenic point sources  
14 (Lourens et al., 2011). However, the relative importance of BC contributions from these  
15 anthropogenic sources in South Africa is still largely unknown and few BC-related papers have  
16 been published in the peer-reviewed public domain. Venter et al. (2012) used BC mass  
17 concentration data collected at the Marikana monitoring station to verify the origin of CO and  
18 PM<sub>10</sub>, but did not consider BC further. Collett et al. (2010) only presented a single diurnal plot  
19 for BC mass concentration measured at the Elandsfontein monitoring station in 2010.  
20 Hyvärinen et al. (2013) used BC mass concentration data collected at the Welgegund  
21 monitoring station to illustrate the use of a newly developed method to correct BC mass  
22 concentration values measured with a multi-angle absorption photometer (MAAP). In addition,  
23 Martins (2009) determined elemental carbon (EC) and organic carbon (OC) mass  
24 concentrations from three two-week winter campaigns and one two-week summer campaign at  
25 two sites, as part of the framework of the Deposition of Biogeochemical Important Trace  
26 Species (DEBITS)-International Global Atmospheric Chemistry (IGAC) in Africa project  
27 (Galy-Lacaux et al., 2003; Martins et al., 2007). However, this data have not yet been published  
28 in the peer-reviewed scientific domain. Maritz et al. (2015) and Aurela et al. (2016) presented  
29 limited EC mass concentration data from some regional background sites in South Africa. Kuik  
30 et al. (2015) used the Weather Research and Forecasting model, including chemistry and  
31 aerosols (WRF-Chem), to analyse the contribution of anthropogenic emissions to the total  
32 tropospheric BC mass concentrations from September to December 2010 in South Africa.  
33 However, significant underestimations and uncertainties with regard to BC mass concentrations

were reported by the afore-mentioned authors.

From the above-mentioned, the need for improved BC mass concentration data for South Africa is evident. This paper presents spatial and temporal assessments of equivalent black carbon (eBC) derived from an optical absorption method and elemental carbon (EC) determined by an evolved carbon method (definitions according to Petzold et al., 2013) mass concentrations over the northern interior of South Africa, as well as potential contributing sources of eBC at Elandsfontein, a site located on the South African Highveld.

## **2 Measurement locations and methods**

### **2.1 Measurement sites**

In this paper, eBC or EC mass concentration data from eight measurement stations are presented. At three of these stations, continuous high resolution eBC measurements were conducted, i.e. Elandsfontein, Welgegund and Marikana, while at the remaining five stations, i.e. Louis Trichardt, Skukuza, Vaal Triangle, Amersfoort and Botsalano, samples were collected once a month on a filter for a period of 24 hours and analysed off-line to yield EC. The locations of these sites within a regional context are indicated in Figure 1. In order to contextualise all the sites, a brief description of each site is presented below.

#### **Insert Figure 1**

##### **2.1.1 Elandsfontein**

The Elandsfontein monitoring station (26.25°S 29.42°E; 1750 m.a.m.s.l.) is located on the top of a hill approximately 200 km east of Johannesburg in the highly industrialised South African Highveld (Collett et al., 2010). The site is relatively frequently affected by plumes from coal-fired power stations, metallurgical smelters and a large petrochemical operation that occur within an approximately 60 km radius around the site (Laakso et al., 2012). The site was used for the European Integrated Project on Cloud Climate, Aerosols and Air Quality Interactions (EUCAARI) project for measurements outside Europe; with state-of-the-art instruments for comprehensive aerosol measurements (Laakso et al., 2012; Kulmala et al., 2009). Measurements were conducted from February 2009 to January 2011 with a PM<sub>10</sub> inlet.

##### **2.1.2 Marikana**

The Marikana monitoring station (25.70°S 27.48°E; 1170 m.a.m.s.l.) is located in a small village situated approximately 35 km east of the city of Rustenburg, in the North West Province of South Africa. Within an approximately 55 km radius from this site there are 11 pyrometallurgical smelters and at least twice as many mines (feeding the afore-mentioned

smelters) (Venter et al., 2012). However, there were no mining and/or industrial activities within a 1 km radius of the site. The closest surroundings included semi-formal (government-built housing developments, mostly with some form of informal housing additions by the occupants) and informal (self-erected, sometimes unauthorised, mostly without municipal services) settlements, a formal residential area with a gas station and shops, as well as tarred and untarred roads serving the communities in this area (Venter et al., 2011; Hirsikko et al., 2012). Measurements were conducted from September 2008 to May 2010 with a PM<sub>10</sub> inlet.

### **2.1.3 Welgegund**

The Welgegund measurement station ([www.welgegund.org](http://www.welgegund.org), 26.57°S 26.94°E, 1480 m.a.m.s.l.) is situated approximately 100 km west of Johannesburg on the property of a commercial farmer. It is representative of a regional background site, but is also affected by aged plumes from major source regions in South Africa (Jaars et al., 2014; Tiitta et al., 2014; Venter et al., 2016). A detailed description of the Welgegund measurement station and related source regions was relatively recently presented by Beukes et al. (2013). Measurements reported in this paper covered the period June 2010 to May 2012. A PM<sub>10</sub> inlet was used from 1 June 2010 to 25 August 2010, as well as 1 September 2011 to 31 May 2012, while a PM<sub>1</sub> inlet was used from 26 August 2010 to 31 August 2011. The PM<sub>1</sub> inlet sampling period was undertaken to better quantify PM<sub>1</sub> aerosol chemical composition, which was reported in a previous paper (Tiitta et al., 2014).

### **2.1.4 DEBITS sites**

Maritz et al. (2015) introduced all the DEBITS sites for which data is presented. Therefore only synopses of the site descriptions, taken from the afore-mentioned paper, are given here. The DEBITS project is an international long-term project that mainly focuses on measuring atmospheric deposition of pollutants (Galy-Lacaux *et al.*, 2003; Mphepya et al, 2004 and 2006; Conradie et al., 2016). The Louis Trichardt (22.99 S 30.02 E; 1300 m.a.m.s.l.), Skukuza (24.99 S 31.58 E; 267 m.a.m.s.l.), Vaal Triangle (26.72 S 27.88 E; 1320 m.a.m.s.l.), Amersfoort (27.07 S 29.87 E; 1628 m.a.m.s.l.) and Botsalano (25.54 S 25.75 E; 1424 m.a.m.s.l.) sites were operated within the afore-mentioned programme. Amersfoort is situated in a grassland biome and is affected by anthropogenic activities on the Mpumalanga Highveld. Louis Trichardt is a rural site that is predominantly used for agricultural purposes within the savannah biome. Skukuza is a regional background site within the savannah biome and is situated in a protected area (Kruger National Park). The Vaal Triangle site is within the

grassland biome and is situated in a highly industrialised area, affected by emissions from various industries, traffic and household combustion. Botsalano is a regional background site that is situated within the savannah biome and a protected area (Botsalano Game Reserve). In this paper EC sampled at these sites with a PM<sub>10</sub> inlet was reported for the period March 2009 to April 2011.

## **2.2 Sampling and analysis methods**

Aerosol BC mass concentration can be measured using both online and off-line methods. In this paper eBC was measured with a light-absorption method and EC with a thermo-optical method (Petzold et al., 2013).

### ***2.2.1 Online sampling and analysis of eBC***

eBC mass concentration was continuously measured at Elandsfontein, Marikana and Welgegund with a Thermo Scientific, Model 5012 Multi-angle Absorption Photometer (MAAP) with time resolutions of 1 minute that was converted to 15 minute averages. The MAAP measures aerosol eBC with a filter-based method that uses a combination of reflection and transmission measurements together with a radiative transfer model to yield eBC concentration (Petzold and Schönlinner, 2004). However, if the automated filter change in MAAP occurs at a high eBC concentration, an artefact may occur (Hyvärinen et al., 2013). In this study, the MAAP eBC measurements were corrected for this artefact according to Hyvärinen et al. (2013). Furthermore, the MAAPs at Welgegund and Elandsfontein were operated at reduced flow rates, which decreased the number of such filter change artefacts.

### ***2.2.2 Off-line sampling and analysis of EC***

Twenty four (24)-hour PM<sub>10</sub> aerosol samples were collected on quartz filters (with a deposit area of 12.56 cm<sup>2</sup>) once a month at Louis Trichardt, Skukuza, Vaal Triangle, Amersfoort and Botsalano for the entire measurement period reported. Sample preparation and analysis were according to the methods described by Maritz et al. (2015). The quartz filters were prebaked at 900°C for four hours and cooled down in a desiccator, prior to sample collection. MiniVol samplers developed by the United States Environmental Protection Agency (US-EPA) and the Lane Regional Air Pollution Authority were used during sampling (Baldauf et al., 2001). In this study, samples were collected at a flow rate of 5 L/min, which was verified by using a handheld flow meter. Filters were handled with tweezers while wearing surgical gloves, as a precautionary measure to prevent possible contamination of the filters. All thermally pre-treated filters were also visually inspected to ensure that there were no weak spots or flaws.



After inspection, acceptable filters were weighed and packed in airtight Petri dish holders until they were used for sampling. After sampling, the filters were again placed in Petri dish holders, sealed off, bagged and stored in a portable refrigerator for transport to the laboratory. At the laboratory the sealed filters were stored in a conventional refrigerator. Twenty four hours prior to analysis, samples were removed from the refrigerator and weighed prior to analysis. Several methods can be used to analyse EC collected on filters (Chow et al., 2001). In this study, the IMPROVE thermal/optical (TOR) protocol (Chow et al., 1993; Chow et al. 2004; Environmental Analysis Facility, 2008; Guillaume et al., 2008) was applied using a Desert Research Institute (DRI) analyser. With this method, the filters are subjected to volatilisation at temperatures of 120, 250, 450 and 550°C in a pure helium (He) atmosphere and at temperatures of 550, 700 and 800°C in a mixture of He (98%) and oxygen (O<sub>2</sub>) (2%) atmosphere. In this process, carbon compounds that are released are converted to CO<sub>2</sub> in an oxidation furnace with a manganese dioxide (MnO<sub>2</sub>) catalyst at 932°C. Then, the flow passed through a digester where the CO<sub>2</sub> is reduced to methane (CH<sub>4</sub>) on a nickel-catalysed reaction surface. The amount of CH<sub>4</sub> formed is detected by a flame ionisation detector (FID), which is converted to carbon mass using a calibration coefficient. The carbon mass peaks detected correspond to the different temperatures at which the seven separate carbon fractions, which include three elemental carbon (EC) fractions, were released. These fractions were depicted as different peaks on the thermogram, of which the surface areas were proportional to the amount of CH<sub>4</sub> detected. The DRI instrument can detect EC as low as 0.1 µg/cm<sup>2</sup>.

### **2.3 Savannah and grassland fire locations**

A number of products can be used to obtain savannah and grassland fire locations. Fire locations presented in this paper were obtained from the remote sensing observations of fires from the MODIS collection 5 burned area product (Roy et al., 2008; MODIS, 2014).

### **2.4 Air mass back trajectory analysis**

The Hybrid Single-Particle Lagrangian Integrated Trajectory (HYSPLIT 2014) model (version 4.8), developed by the National Oceanic and Atmospheric Administration (NOAA) Air Resources Laboratory (ARL) was used to calculate air mass histories (Draxler and Hess, 2004). Meteorological data from the GDAS archive of the National Centre for Environmental Prediction (NCEP) of the United States National Weather Service (USNWS) and archived by the ARL (Air Resources Laboratory, 2014a), was used as input. This data has a 40 or 80 km grid resolution, depending on the year considered (NASA, 2015), with all the data used in this

study having 40 km grid resolution. All trajectories were calculated for 24 hours backwards, to arrive on the hour at an arrival height of 100 m above ground level. An arrival height of 100 m was chosen, since the orography in HYSPLIT is not well defined, which could result in increased error margins on individual trajectory calculations if lower arrival heights are used (Air Resources Laboratory, 2014c). For such calculated back trajectories, maximum error margins of 15 to 30% of the trajectory distance travelled have been estimated (Stohl, 1998; Riddle et al., 2006; Vakkari et al., 2011).

## **2.5 Linking ground-based measurements with point sources using back trajectories**

This method was introduced by Maritz et al. (2015) who used it to link ambient organic carbon (OC) and EC concentrations to potential sources. The same method was applied here, to assess if large point sources and in- or semi-formal settlements contributed to ambient eBC concentrations at the sites where active eBC data was gathered (Elandsfontein, Welgegund and Marikana). The method was not applied to sites where 24-hour composite EC samples were taken (Louis Trichardt, Skukuza, Vaal Triangle, Amersfoort and Botsalano). The method relates eBC concentrations measured at a particular sampling site with the closest distance between the hourly arriving trajectory and the afore-mentioned sources (large point sources, as well as in- and semi-formal settlements). Figure 2 presents an illustration of the method applied for a specific sampling site to determine the shortest distance between a 24-hour back trajectory and large point sources. The distances between the large point sources (indicated by the black markers) and a specific back trajectory were calculated for each of the hourly locations of the 24-hour back trajectory (indicated by the red dots on Figure 2). The red line indicates the shortest distance between hourly locations of this specific trajectory and large point sources (i.e. petrochemical operations, coal-fired power stations and pyro-metallurgical smelters). The weaknesses of the afore-mentioned method were that downwind point sources and/or in- or semi-formal settlements, very close to the monitoring site, could in some instances be the closest point source/in- or semi-formal settlements. Additionally, dilution due to distance travelled by the trajectories was not considered.

### **Insert Figure 2**

## **2.6 Determining the relative contribution of eBC from sources**

In order to determine the relative strength of eBC mass concentration sources, detailed correlation analyses were performed for eBC peaks. For instance, it is well known that plumes from coal-fired power stations on the Mpumalanga Highveld are characterised by a

simultaneous increase in NO, NO<sub>2</sub> and SO<sub>2</sub> concentrations (Collect et al., 2010; Lourens et al., 2011). Figure 3 shows the eBC, SO<sub>2</sub>, NO<sub>2</sub>, NO and H<sub>2</sub>S data measured on 14 February 2009. In this figure, it is evident that two well-defined coal-fired power plant plumes were observed between 09:15 and 11:30 based on SO<sub>2</sub>, NO<sub>2</sub> and NO time series, as well as between 18:00 and 21:00. However, both of these coal-fired power plant-associated plumes did not raise the baseline eBC meaningfully. There was, however, a significant eBC plume between 02:00 and 08:30, which coincided perfectly with a simultaneous increase in H<sub>2</sub>S. This eBC plume was therefore associated with the source that emitted the H<sub>2</sub>S. For each such plume the excess eBC ( $\Delta$  eBC) was determined, with the baseline defined as the linear line between the start end eBC concentrations of the observed plume and  $\Delta$  eBC defined as the eBC concentration above the baseline, as indicated in the top pane of Figure 3.

### Insert Figure 3

## 2.7 Multiple linear regression analysis

Several techniques were applied in this paper to characterise possible sources of eBC mass concentrations measured at the various stations, e.g. seasonal patterns, diurnal patterns, back trajectory analyses, and identifying sources based on coincidental increases in species time series. In an attempt to further critically evaluate deductions made from these methods, multiple linear regression (MLR) analyses were conducted. Linear regression is denoted by constants or known parameters (c), an independent variable (x) and a dependent variable (y) by fitting a linear equation to the observed data. MLR is characterised by more than one independent variable (x). In MLR, the relationship between the dependent variable (y) and independent variables (x) is denoted by Equation 1.

$$y = c_0 + c_1x_1 + c_2x_2 + c_3x_3 + \dots + c_zx_z \quad \text{Eq. 1}$$

In this study, MLR was used to determine an equation for the dependent variable eBC. MLR was used to determine the optimum combination of independent variables to derive an equation that could be used to calculate eBC concentrations. Root mean square error (RMSE) was used to compare the calculated values with the measured values. Several authors have previously applied similar methods for various atmospheric species (e.g. Awang et al., 2015; Du Preez et al., 2015; Venter et al., 2015).

## 3 Results and discussions

### 3.1 Spatial variation

In Figure 4, a box and whisker plot indicating the statistical eBC or EC mass concentrations for

each of the sites is presented. The significant difference in number of samples (N) is due to the fact that at the DEBITS sites EC mass concentrations were only measured once per month over a 24-sampling period, whereas at the other sites, one-minute eBC data were collected that were converted to 15 min averages. Precaution should also be taken when directly comparing eBC and EC, since it was previously proven that eBC and EC concentrations can differ by up to a factor of 7 among different methods, with a factor of 2 differences being common (Watson et al., 2005). However, an unpublished 12 month intern-comparison of eBC and EC at the Welgegund measurement site, with the actual sampling and analysis equipment used to acquire data for this study, proved that EC and eBC were within the same order of magnitude (Sehloho, 2017). Therefore, notwithstanding the limitations in directly comparing EC and eBC data, Figure 4 gives the most realistic spatial perspective for the northern interior of South Africa, especially within the context of very little other data being available in the peer reviewed public domain.

#### **Insert Figure 4**

Of all the sites considered, the highest mass concentrations were measured at Vaal Triangle that had a median EC of  $3.2 \mu\text{g}/\text{m}^3$  and a mean of  $4.4 \mu\text{g}/\text{m}^3$  for the entire measurement period. Although sources will be considered in greater detail later, the higher EC mass concentration levels at Vaal Triangle can be attributed to various possible sources. Firstly, this area is densely populated with large semi-formal and informal settlements. This indicates that household combustion for space heating and cooking could be a significant source of EC. Secondly, the area experiences relatively higher traffic volumes and several large point sources (including petrochemical and related chemical industries, two coal-fired power stations and numerous metallurgical smelters) occur in the area. Thirdly, the site experiences less dilution due to the close proximity of the sources to the measurement site that contribute to the observed elevated levels of EC mass concentration.

The eBC at Elandsfontein, as well as the EC at Marikana and Amersfoort sites indicated similar levels with median and mean values of 0.8 and 1.3, 1.2 and 1.7, and 1.1 and  $1.4 \mu\text{g}/\text{m}^3$  respectively. Elandsfontein and Amersfoort lie within the well-known  $\text{NO}_2$  hotspot over the Mpumalanga Highveld identified from satellite observations (Lourens et al., 2012) and are therefore likely to be influenced by industrial activities in this area. Marikana can be affected by household combustion from in- and semi-formal settlements that are located close to the measurement site, as well as the large pyrometallurgical sources occurring in the area (Venter

et al., 2012; Hirsikko et al., 2012).

The background sites, i.e. Welgegund, Botsalano, Louis Trichardt and Skukuza had lower eBC or EC levels compared to other locations, with median and mean concentrations of 0.4 and 0.7, 0.7 and 0.9, 0.8 and 0.9, and 0.9 and 1.1  $\mu\text{g}/\text{m}^3$ , respectively. All these background sites are likely to be affected most by regional savannah and grassland fires that are common in southern Africa or by pollutants transported from other parts of the country. However, Welgegund, which is the furthest west of these sites, is likely to be affected less by savannah and grassland fires due to the dryer biomes, i.e. the Kalahari and Karoo that are located to the west of this site. These drier biome regions produce less biomass that can burn (Mafusire et al., 2016). It is therefore understandable that Welgegund had lower eBC levels than the other background sites. Obviously, Elandsfontein, Marikana, Vaal Triangle and Amersfoort will also be affected by regional savannah and grassland fires, in addition to the possible sources already mentioned.

The eBC and EC concentrations presented for all the sites considered (Figure 4) should also be contextualised. The background site with the lowest  $\text{PM}_{10}$  eBC concentrations reported here, i.e. Welgegund, had similar or higher eBC mass concentration values than typical western European background sites. BC mass concentrations of less than 0.2 to 0.3  $\mu\text{g}/\text{m}^3$  have been reported for western parts of northern Europe (e.g. Yttri et al., 2007). At natural and rural European background sites, values of 0.3 to 0.5 and 0.6 to 1.6  $\mu\text{g}/\text{m}^3$  have been reported, respectively (e.g. Putaud et al., 2004; Hyvärinen et al., 2011). The other South African background sites reported here, i.e. Botsalano, Louis Trichardt and Skukuza, had higher mean and median values than the afore-mentioned European background/natural sites. The industrial/urban/household affected sites reported here, i.e. Elandsfontein, Marikana, Vaal Triangle and Amersfoort had higher average eBC or EC mass concentration levels than, for instance, an urban site in a large European city, where BC mass concentrations had an average of approximately 1.0  $\mu\text{g}/\text{m}^3$  (Järvi et al., 2008; Viidanoja et al., 2002). In general, it can therefore be stated that eBC or EC mass concentrations across the measurement area considered are relatively high.

Apart from the spatial information and possible indication of contributing sources obtained from Figure 4, it is also evident from the comparison of the  $\text{PM}_1$  and  $\text{PM}_{10}$  eBC data of Welgegund that most of the eBC resides in the  $\text{PM}_1$  size fraction, which was expected.

## **3.2 Temporal variations**

### **3.2.1 Seasonal variations**

In order to determine seasonal patterns, only the site where continuous measurements were conducted was considered. Monthly statistical distributions of eBC mass concentrations for Elandsfontein, Welgegund and Marikana measurement sites are presented in Figure 5. As is evident from these figures, there is a distinct and similar seasonal pattern observed at all three sites, with the highest eBC mass concentrations measured in June to October. These months coincide with the colder winter months of June to August, as well as the dry season on the South African Highveld occurring between May and middle October. Venter et al. (2012) previously indicated that household combustion for cooking and space heating in informal and semi-formal settlements during winter could be a significant eBC mass concentration source on a local scale. However, it has not yet been determined whether such household combustion could also make a significant regional contribution in South Africa. During the dry season, increased savannah and grassland wild fires occur, which contributed to increased atmospheric eBC concentrations (Bond et al., 2004, Saha and Despiu, 2009). The influence of both of these potential eBC sources, i.e. household combustion and wild fires, will be discussed later in Section 3.3. Obviously, increased atmospheric stability during the colder months (Garstang et al., 1996) will also lead to trapping of low level emissions, hence resulting in possible higher eBC concentrations. This is discussed in greater detail in the next section.

**Insert Figure 5**

### **3.2.2 Diurnal variations**

Average diurnal plots as well as average seasonal diurnal plots (separate for summer, autumn, winter and spring) for the stations where continuous eBC mass concentration data were gathered, i.e. Elandsfontein, Marikana and Welgegund (both PM<sub>1</sub> and PM<sub>10</sub>), are presented in Figure 6.

**Insert Figure 6**

The Elandsfontein diurnal plots indicate that the main source of eBC is not high stack emissions. The area in which Elandsfontein is situated, is a well-known international NO<sub>2</sub> hotspot, with tropospheric column densities similar to what is observed over south-east Asia (Lourens et al., 2012; Lourens et al., 2016). It is widely accepted that NO<sub>2</sub> in this hotspot mainly originates from NO<sub>x</sub> emission from coal-fired power stations. The troposphere over the Highveld is strongly layered, with several inversion layers occurring. These layers prevent vertical mixing

1 to a large degree (Garstang et al., 1996). The afore-mentioned  $\text{NO}_x$  emission are released into  
2 the atmosphere via high stacks, which are typically taller than 300m. The effective stack heights  
3 (actual stack heights plus rise due to emissions being hot) were designed to ensure that the  $\text{NO}_x$   
4 emissions are released above the lowest inversion layers, to prevent excessive local pollution  
5 and ensure distribution over a wider area. Collet et al. (2010) proved that  $\text{NO}_2$  concentrations  
6 at Elandsfontein peak after 11:00 am, due to the breakdown of the lowest inversion layers,  
7 which allow downward mixing of the  $\text{NO}_x$  tall stack emissions. Therefore, if eBC mainly  
8 originated from these large point sources with tall stacks, eBC concentrations would also have  
9 peaked, after the breakdown of the night-time inversion layers that would allow downward  
10 mixing of tall stack emitted eBC. However, this is clearly not the case. Additionally, the winter  
11 diurnal plot for Elandsfontein indicates substantially higher values during night-time when the  
12 planetary boundary layer (PBL) is less well mixed (i.e. strong low level inversion layers that  
13 trap surface emissions), which re-enforces the notion that the major origin of eBC is from low-  
14 level sources, rather than industrial high stacks. At Elandsfontein the daily evolution of the  
15 PBL starts approximately three to four hours after sunrise (varies between 05:07 and 06:56 local  
16 time), which results in increasing atmospheric mixing down from the upper troposphere,  
17 including high stack emissions (Korhonen et al., 2014). Considering all the afore-mentioned,  
18 the most likely eBC sources during winter (June to August) and the dry season (May to middle  
19 October) are surface emissions from household combustion, and savannah and grassland fires.  
20 This is an important finding, since industries on the Mpumalanga Highveld are often blamed for  
21 all forms of pollution, due to the  $\text{NO}_2$  hotspot over this area.

22 In contrast to Elandsfontein, eBC concentrations at Marikana peaked in the early mornings  
23 (05:00-09:00) and again in the early to late evenings (17:30-22:00). These times correlate with  
24 the peak times for household combustion for space heating and cooking in the nearby in- and  
25 semi-formal settlements (Venter et al. 2012). Seasonal timing of the peak eBC concentration  
26 in the diurnal plots confirms that household combustion is the main source at this site. In winter,  
27 during which time daylight hours are shorter, the peak morning eBC concentration is at ~07:00  
28 and the evening peak at ~18:00; whereas, during summer, with longer daylight hours, the peak  
29 morning eBC concentration is at ~06:00 and the evening peak at ~20:00. During the cold winter  
30 months, space heating is a priority, apart from cooking, while in summer, household combustion  
31 would mainly be used for cooking. These seasonal household combustion use patterns are  
32 reflected by the diurnal eBC patterns for Marikana.

The eBC diurnal plots of Welgegund do not indicate well-defined peaks as observed for Marikana. This is expected, since there are no semi- or informal settlements located close to the Welgegund station. Additionally, there are also no large point sources close to Welgegund, as there are at Elandsfontein. Therefore, only sources that have a regional influence are likely to affect eBC levels at Welgegund. It is therefore likely that savannah and grassland fires, especially in the winter and early spring, are mainly responsible for eBC levels measured at Welgegund and mainly long-range transportation during the wet season. The lower PBL during the evenings and early mornings will concentrate the eBC and contribute to eBC levels rising in the evening and only decreasing three to four hours after sunrise, as suggested by Korhonen et al. (2014). This effect is strongest in the winter months.

### **3.3 eBC source identification**

#### *3.2.1 General*

As has already been indicated, there are various possible sources for eBC, e.g. industrial, household combustion, traffic, and savannah and grassland fires. In this section, possible significant contributing sources are considered further. Figure 7 indicates the fire pixel counts calculated from MODIS (collection of 5 burned area product) (Roy et al., 2008) within the entire southern Africa (10-35°S and 10-41°E) indicated on the primary y-axis, as well as fire pixel counts within a radius of 125 km around measurement sites where high resolution eBC data was gathered on the secondary y-axis.

#### **Insert Figure 7**

It is important to note that it is difficult to separate the influence of various sources at a specific site, since the measured eBC originates from a mixture of contributing sources. Therefore, Figure 7 was considered first, since it provided guidance about which periods would be best to consider for the different sources. For instance, there are very few savannah and grassland fires during December to February every year in the northern interior of South Africa. The savannah and grassland fires that do occur during this period occur in the southern Western Cape, which will not influence eBC levels in the northern interior significantly. In addition, minimal household combustion for space heating takes place in December to February, since it is the warmest months. During this time household combustion for cooking will still take place, but such daily emission periods are far shorter than the extended space heating period (typically early evening, throughout the night, until after sunrise the next day) occurring during the colder months. Considering the afore-mentioned, it is best to isolate industrial and traffic related eBC



sources during December to February.

It is clear for the overall southern African fire frequencies, as well as those around each site (Figure 7) that August and September have the highest savannah and grassland fire intensities. This is the driest period, just before the onset of the first rains, usually in middle October. We can therefore isolate savannah and grassland fires best in this period, since its effect is strongest. The influence of household combustion is also not that strong in this period; since it is already becoming warmer and therefore less space heating is required. By considering aerosol particle concentrations at Marikana, Vakkari et al. (2013) proved that the evening peak associated with household combustion was significantly lower in September than in June to July.

Since it is coldest in June and July, the effect of household combustion for space heating is at its strongest, making the isolation of the household combustion effect better during these months.

In the following sections, eBC contributions from the above-mentioned sources, i.e. industrial, traffic, savannah and grassland fires, and household combustion, will be explored in greater detail for the Elandsfontein site only. This site was chosen, since it can be affected by all the afore-mentioned sources, while the other sites where continuous high resolution data were gathered will mainly be influenced by savannah and grassland fires (Welgegund) or household combustion (Marikana).

### *3.3.2 Industrial contribution to eBC at Elandsfontein*

Numerous large industrial point sources linked to coal utilisation occur in the South African interior, e.g. coal-fired power stations that produce most of South Africa's electricity, large petrochemical operations utilising coal gasification and numerous pyro-metallurgical smelters utilising coal and coal-related products as carbonaceous reductants for the production of various steels and alloys (Collet et al., 2010; Lourens et al., 2011; Beukes et al., 2012). However, the possible contributions of these large point sources to atmospheric BC have not yet been investigated.

In Figure 8, eBC concentrations measured at Elandsfontein were plotted against the shortest distances that back trajectories passed any large point source, during the summer months (December to February), when minimal household combustion, as well as savannah and grassland fires occur. Although there was no clear correlation (Figure 8), the results indicated that at least some trajectories passing closer to these large industrial point sources had higher eBC concentrations. This suggests that eBC contributions from large industrial point sources

cannot be ignored, notwithstanding the diurnal patterns, indicating that high stack industrial emissions were not the main source (Figure 6).

### **Insert Figure 8**

Although indicated in Section 3.2.2 that it was unlikely that high stack emissions were the main source of eBC at Elandsfontein, the possible fractional contributions of industries still need to be assessed. In order to quantify this, eBC peaks that coincided with peaks of other pollutants, which are characteristic of large point sources in that area, were considered for the December to February period. Two distinct types of contributing sources were identified, i.e. eBC peaks that coincided with SO<sub>2</sub>, NO<sub>2</sub> and NO, as well as eBC peaks that only coincided with H<sub>2</sub>S. From literature, it is known that plumes from coal-fired power plants on the South African Highveld are characterised by coincidental SO<sub>2</sub>, NO<sub>2</sub> and NO increases (Collet et al., 2010; Lourens et al., 2011). Although it is not shown here, eBC plumes that were associated with these species were confirmed to have originated from coal-fired power stations with back trajectory analyses. However, H<sub>2</sub>S peaks that coincided with the eBC peaks could have been from various sources, e.g. the large petrochemical plant near Secunda, pyro-metallurgical smelters in the area or smouldering coal dumps that burn as a result of spontaneous combustion. In order to identify the origin of the eBC peaks that were associated with H<sub>2</sub>S only, a map on which all back trajectories that arrived at Elandsfontein during these eBC peaks (coincidental increases in eBC and H<sub>2</sub>S) were plotted, is presented in Figure 9, together with a wind rose for such events. From these figures, it is evident that the back trajectories that were associated with simultaneous eBC and H<sub>2</sub>S concentration peaks only passed over the sector between the northwest and northeast from Elandsfontein. This is the area where all the pyro-metallurgical smelters are located. Smouldering coal dumps occur in all directions from Elandsfontein. Additionally, no trajectories associated with coincidental eBC and H<sub>2</sub>S increases had passed over the petrochemical operation. It therefore seems likely that the eBC contribution associated with H<sub>2</sub>S originates from the pyro-metallurgical smelters in the sector located between northwest and northeast from Elandsfontein.

### **Insert Figure 9**

#### *3.3.3 Traffic contribution to eBC at Elandsfontein*

From literature, it seems feasible to associate increased BC concentrations with traffic emissions, particularly diesel-powered vehicles (Cachier, 1995; Cooke and Wilson, 1996; Bond and Sun, 2005). The Mpumalanga Highveld around Elandsfontein is the area where most

thermal coal is mined in South Africa, which is mostly transported by diesel trucks via various roads criss-crossing the area as indicated in Figure 10a. However, the closest tarred road, i.e. the R35, passes Elandsfontein approximately 4.7 km to the east. This road is also one of the most utilised for coal road transportation. Additionally, to the north of Elandsfontein, numerous such tarred roads are located, e.g. the national N12 and N4 highways pass Elandsfontein approximately 38 km to the north and north-west. It therefore seems reasonable that the traffic-related eBC back trajectory map (Figure 10a, which was for coincidental increases in eBC and NO<sub>2</sub> time periods only) is somewhat biased toward the east and north, although limited contributions from other sectors are also evident. The wind rose showing the prevailing wind direction during periods when eBC plumes that coincided with NO<sub>2</sub> plumes were observed (Figure 10b) also indicates the sources to be mainly from the east, i.e. where the R35 passes Elandsfontein.

#### **Insert Figure 10**

##### *3.3.4 Household combustion contribution to eBC at Elandsfontein*

Venter et al. (2012) indicated that household combustion for space heating and cooking in in- and semi-formal settlements contributes significantly to poor air quality in such settlements. In Figure 11, the relationships between monthly average and median eBC, against monthly mean and median temperatures for Elandsfontein, are presented. As is evident from the results presented in Figure 11, there is a significant correlation between eBC concentration and temperature, if August and September are ignored (indicated with hollow markers in Figure 11). During these months, significant eBC contributions can be expected from savannah and grassland fires (see Figure 7). The correlation between eBC concentration and temperature indicates that household combustion for space heating contributes significantly to eBC levels measured at Elandsfontein, especially during the colder months when household combustion is used more frequently for space heating.

#### **Insert Figure 11**

Similar to the analysis performed for the large industrial point sources (Figure 8), eBC concentrations were drawn as a function of the closest distance that back trajectories had passed in- and semi-formal settlement for Elandsfontein. However, this was done only for the winter months of June and July for both years, since household combustion contributions could then be better isolated from savannah and grassland fire contributions during these periods. These results are presented in Figure 12. Although not conclusive, the results presented indicate that,

1 in general, higher eBC concentrations were observed when trajectories passed closer to in- and  
2 semi-formal settlements in June and July.

### 3 **Insert Figure 12**

4 Household combustion results in the emission of a number of different species (Venter et al.,  
5 2012). In this work tracers for household combustion were determined from species that  
6 simultaneously increased with eBC, including NO<sub>2</sub>, SO<sub>2</sub> and H<sub>2</sub>S, but not NO. Low-grade coal  
7 that is burned in ineffective stoves is commonly used for household combustion in the  
8 Mpumalanga Highveld, due to such coal being relative inexpensive. The use of which results  
9 in NO<sub>x</sub>, SO<sub>2</sub> and H<sub>2</sub>S emissions. During the cold winter months of June and July, strong  
10 inversion layers trap pollutants emitted closer to ground level and prevent the mixing and  
11 subsequent transportation of these pollutants. The low-level emissions from in- and semi-  
12 formal settlements are therefore not dispersed before the inversion layers break up in mid-  
13 morning. A previous study has indicated that the PBL starts growing around 10:00 local time  
14 at Elandsfontein during the winter months (Korhonen et al., 2014). It can therefore be accepted  
15 that the low-level inversion layers also start dissipating at that time. The long residence time  
16 of air masses around in- and semi-formal settlements in winter before being dispersed, as well  
17 as additional transport time, results in NO being oxidised to NO<sub>2</sub> prior to these plumes being  
18 measured at Elandsfontein.

19 Figure 13a indicates back trajectories associated with household combustion contribution to  
20 eBC levels (for time periods with coincidental increases in eBC with NO<sub>2</sub>, SO<sub>2</sub> and H<sub>2</sub>S, but  
21 not NO). Most of these back trajectories passed over the Thubelihle and Kriel settlements,  
22 which are located 12.4 and 13.8 km from Elandsfontein, respectively. Apart from this relatively  
23 local eBC influence from household combustion, most trajectories associated with household  
24 combustion eBC plumes passed over the sector between east and north-north-east, where the  
25 cities of Witbank and Middelburg, as well as the Johannesburg-Pretoria mega-city are located.  
26 These larger cities have many more large in- and semi-formal settlements associated with them  
27 than the smaller towns in the area do. The wind rose showing the prevailing wind direction  
28 during periods when eBC plumes that coincided with NO<sub>2</sub>, SO<sub>2</sub> and H<sub>2</sub>S plumes were observed  
29 (Figure 13b) also indicates the sources to be mainly from more or less the same direction as  
30 most of the back trajectories.

### 31 **Insert Figure 13**

### 3.3.5 *Savannah and grassland fire contribution to eBC at Elandsfontein*

Vakkari et al. (2014) relatively recently indicated how savannah and grassland fire emission aerosols are changed via atmospheric oxidation in South Africa. To positively identify savannah and grassland fire plumes, the afore-mentioned authors used CO and eBC as coincidental increasing species. However, CO was not measured at Elandsfontein and therefore the positive identification of savannah and grassland plume could not be undertaken using this method. Additionally, the plumes of savannah and grassland fires occurring in neighbouring countries arriving at Elandsfontein will be diluted and aged. Such regional fires lift the entire eBC baseline, rather than exhibiting well-defined plumes that can be separated from the baseline (Mafusire et al., 2016), as was done for the industrial, traffic and household combustion sources. Thus far in the paper, we have considered August and September as the months in which savannah and grassland fires frequencies peak. However, some household combustion might still occur in August. Therefore, to determine the overall baseline increase as a result of savannah and grassland fires, only September was considered as being representative of savannah and grassland fires, while the summer months (December to February) can be considered as the baseline. By subtracting the September eBC mean from the summer mean, the eBC baseline increased by  $2.01 \mu\text{g}/\text{m}^3$ . This increase will be contextualised with the previously investigated sources in the next section.

### 3.3.6 *Contextualisation of eBC source strengths at Elandsfontein*

Up to now, the individual eBC sources for Elandsfontein were discussed, but their strengths were not compared with one another. In Figure 14, the comparison of the  $\Delta$  eBC from coal-fired power stations, pyro-metallurgical smelters, traffic, household combustion, as well as savannah and grassland fires for Elandsfontein is presented. The relative savannah and grassland fire source strength is not statistically presented with a box and whisker as for the other sources, but only with a black star that indicates the mean eBC baseline increase during September if compared to the summer months of December to February. The data presented in Figure 14 were normalised to account for variations in PBL height at Elandsfontein. This was done by using the monthly average PBL daily maximum heights reported by Korhonen et al. (2014) for 2010 at Elandsfontein. Unfortunately no such data existed for 2009, therefore the 2009 monthly PBL heights were assumed to be similar to 2010. Thereafter the ratios of the average PBL daily maximum heights for each of the periods during which certain sources could be better isolated (i.e. December to February for large point sources and traffic emission; June to July to household combustion) were calculated, compared to the average PBL daily

1 maximum heights for August and September (period with peak savannah and grassland fire  
2 occurrence). The  $\Delta$  eBC for each of the sources identified in the December to February, as well  
3 as June to July periods were then adjusted with these ratios to account for variations in the  
4 PBL, which could have a significant dilution or concentration effect on the measured eBC  
5 values, from which the  $\Delta$  eBCs were derived. The results indicate the significant source strength  
6 of household combustion, as well as savannah and grassland fires, as measured at Elandsfontein.  
7 However, coal-fired power stations, pyro-metallurgical and/or char plants and traffic contribute  
8 year round, while household combustion, as well as savannah and grassland fires only  
9 contribute significantly in May to August, and June to September, respectively. Bond et al.  
10 (2013) indicated relatively high BC emissions from biofuel cooking (calculated for Africa in  
11 total), but did not indicate space heating to contribute significantly. However, our data seem to  
12 prove that space heating does contribute meaningfully to eBC levels in South Africa during the  
13 colder winter months (June-July).

#### 14 **Insert Figure 14**

15 Vakkari et al (2014) used  $\Delta$  eBC in relation to other species to characterise differences in plumes  
16 of savannah and grassland fires. In a similar manner, these ratios for  $\Delta$  eBC divided by species  
17 that were characteristic of the different plume types identified (i.e. representing industrial,  
18 traffic or house hold combustion) were determined and are presented in Figure 15. Since so  
19 little BC data is available for South Africa, the median and/or mean values indicated in this  
20 figure could be used in subsequent modelling studies as emission factors to estimate eBC if  
21 only the concentration(s) of the species that were used in calculating these ratios are known.

#### 22 **Insert Figure 15**

### 23 **3.4 Mathematical confirmation of eBC sources at Elandsfontein**

24 Four scenarios were investigated with MLR analyses. Firstly, MLR analysis was conducted for  
25 the entire monitoring period at Elandsfontein. As is evident from the top left pane in Figure 16,  
26 the RMSE difference between the actual measured eBC concentration and the calculated eBC  
27 concentrations if only one independent parameter was included in the optimum MLR solution  
28 was approximately 1.54. The RMSE difference could be reduced by including more  
29 independent parameters in the optimum MLR solution. However, it was found that the  
30 inclusion of more than nine independent parameters did not further reduce the RMSE difference  
31 significantly.

#### 32 **Insert Figure 16**

From the MLR analysis conducted for the entire measurement period at Elandsfontein, the actual MLR equation could be obtained, which is presented as Equation 2. With this equation, eBC at Elandsfontein could be calculated. The comparisons between actual and calculated (with Equation 2) eBC concentrations are presented in Figure 17. From this comparison, it is evident that Equation 2 could be used to calculate eBC at Elandsfontein relatively accurately.

$$y = -33.7038 + (0.0050 \times O_3) + (0.0387 \times SO_2) + (0.0006 \times NO_2) + (0.0722 \times H_2S) + (-0.0174 \times RH) + (0.0997 \times WS) + (0.0005 \times WD) + (0.0421 \times P) + (2.27433 \times T\text{-grad}) \quad \text{Eq. 2}$$

### **Insert Figure 17**

In order to use MLR to verify whether the eBC contribution sources were identified correctly in Section 3.3, MRL analyses were also conducted for the different time periods defined for isolation of the various sources, i.e. December to February for industrial and traffic sources, June and July for household combustion, and August and September for savannah and grassland fires.

As is indicated in Equation 3 and the top right pane of Figure 16, the optimum MLR solution obtained for the December to February period included seven independent variables in the equation. Firstly, the fact that fewer independent variables were required to reduce the RMSE optimally, if compared with the overall period (top left pane of Figure 16), indicates that the December to February period is influenced by fewer sources. Secondly, the identity of the independent variables and the sign (positive or negative) associated with them in Equation 3 are noteworthy. Increased  $O_3$  concentrations led to lower eBC, which indicates that aged air masses had lower eBC than fresh plumes do. This supports the notion that relatively nearby industry and traffic sources dominate. The increased eBC, associated with increased  $NO_2$  and  $H_2S$  concentrations in Equation 3, supports the identity of the specific source types previously identified, i.e. coal-fired power stations, pyrometallurgical smelters, as well as traffic emissions. The remaining independent variables in Equation 3 are associated with meteorological parameters, which could indicate that meteorological patterns (e.g. atmospheric stability as indicated by T-gradient) could have a significant influence on plumes containing eBC measured at Elandsfontein.

$$y = -30.3494 + (-0.0170 \times O_3) + (0.0002 \times NO_2) + (0.1005 \times H_2S) + (0.1350 \times T) + (0.0102 \times RH) + (0.0338 \times P) + (1.8185 \times T\text{-gradient}) \quad \text{Eq. 3}$$

For the June and July periods, Equation 4 and the lower left pane of Figure 16 indicate that the

optimum MLR solution included only four independent variables in the equation. This low number of independent variables confirm that this time period was dominated by a much less complicated source mixture than the overall time period. During June to July, it was previously indicated that household combustion dominated eBC contributions, which is confirmed by the SO<sub>2</sub>- and NO<sub>2</sub>-associated eBC increases indicated by Equation 4. As stated earlier, the household combustion plumes measured at Elandsfontein are likely to be NO depleted, due to the stagnant nature of air masses during the evening and early morning that result in the oxidation of NO to NO<sub>2</sub>. This phenomenon is also indicated by Equation 3. Lastly, increased RH will be associated with increased moisture-induced particle growth that could result in quicker aerosol deposition and therefore reduced eBC levels.

$$y = 1.7061 + (0.0453 \times \text{SO}_2) + (-0.1059 \times \text{NO}) + (0.0855 \times \text{NO}_2) + (-0.0191 \times \text{RH}) \quad \text{Eq. 4}$$

For the August and September periods, Equation 5 and the lower right pane of Figure 16 indicate that the optimum MLR solution included eight independent variables in the equation. Although not as low as for the June and July period, this low number of independent variables confirms that the August and September periods were less complicated than the overall time period. According to Equation 5, increased O<sub>3</sub> for August to September had a positive constant associated with it, which indicates that aged savannah and grassland fire plumes increase the eBC concentrations, while the NO<sub>2</sub> and SO<sub>2</sub> positive constant associations and the negative NO constant association indicate that household combustion still makes contributions during this time. This makes sense, since August is still regarded as a winter month with significant household combustion for space heating taking place. However, since the August and September periods already include warmer spring months (September for both years) with lower household combustion, the H<sub>2</sub>S, T, RH and T-grad relationships observed in summer also already make a meaningful contribution.

$$y = -2.549 + (0.0511 \times \text{O}_3) + (0.0316 \times \text{SO}_2) + (-0.5737 \times \text{NO}) + (0.1840 \times \text{NO}_2) + (0.0433 \times \text{H}_2\text{S}) + (0.0469 \times \text{T}) + (0.0145 \times \text{RH}) + (2.4877 \times \text{T-grad}) \quad \text{Eq. 5}$$

#### 4 Summary and Conclusions

This paper presents the most comprehensive eBC spatial and temporal, as well as source contribution assessments for the South African interior that has been published in the peer-reviewed public domain to date. Limited EC data was also presented, which expanded the overall spatial extent covered in the paper.

Analyses of eBC and EC spatial concentration patterns at eight sites indicate that concentrations



1 in the South African interior are in general higher than what has been reported for the developed  
2 world, e.g. Western Europe. The highest levels were observed at Vaal Triangle, which were  
3 attributed to EC emissions from household combustion emanating from in- and semi-formal  
4 settlements, as well as traffic and large points sources. eBC or EC levels at Elandsfontein,  
5 Amerfoort and Marikana were similar, but likely originated from different sources.  
6 Elandsfontein and Amersfoort lie within the well-known NO<sub>2</sub> hotspot over the Mpumalanga  
7 Highveld and are therefore likely to be influenced by industrial activities in this area, while  
8 Marikana is in close proximity to in- and semi-formal settlements. The background sites, i.e.  
9 Welgegund, Botsalano, Louis Trichardt and Skukuza had lower eBC or EC levels. All these  
10 background sites are likely to be affected most by regional savannah and grassland fires, which  
11 are common in southern Africa.

12 Similar seasonal patterns were observed at all three sites where high resolution eBC data were  
13 collected, i.e. Elandsfontein, Marikana and Welgegund, with the highest eBC concentrations  
14 measured in June to October. These months coincide with the cold winter months of June to  
15 August that indicate possible contributions from household combustion, as well as the dry  
16 season on the South African Highveld occurring between May and mid-October, which  
17 indicates contributions from savannah and grassland fires.

18 Diurnal patterns indicated that at Elandsfontein industrial high stack emissions were not the  
19 most significant source, since no peaks were observed after the breakup of lower-level inversion  
20 layers. The diurnal patterns at Marikana revealed household combustion for space heating and  
21 cooking to be the most significant sources. At Welgegund, the most significant source  
22 contributions were most likely regional savannah and grassland fires.

23 Possible contributing eBC sources were explored in greater detail for Elandsfontein only.  
24 Industrial sources could be isolated best during the summer months of December to February,  
25 since very few savannah and grassland fires, as well as household combustion for space heating  
26 occur then. Coincidental plumes of SO<sub>2</sub>, NO<sub>2</sub>, NO and eBC were used to identify plumes from  
27 coal-fired power stations, while coincidental increases of H<sub>2</sub>S and eBC characterised eBC  
28 contributions from pyrometallurgical smelters. During summer, coincidental increases of NO<sub>2</sub>  
29 and eBC were used to identify traffic emissions. The contribution of household combustion  
30 was isolated during the coldest winter months of June and July. Coincidental increases of NO<sub>2</sub>,  
31 SO<sub>2</sub> and H<sub>2</sub>S, with eBC, which did not correlate to NO increases, were found to characterise  
32 household combustion plumes. Back trajectory analyses and wind roses supported the validity

of all the aforementioned source associations. Savannah and grassland fire plumes could not be isolated since CO was not measured at Elandsfontein. However, the general baseline increase in eBC levels between September (the peak fire frequency period) and the summer months (with virtually no savannah and grassland fires) could be calculated and attributed to savannah and grassland fire eBC emissions. At Elandsfontein, the eBC concentration in September was comparable to the eBC concentration in June to July, which indicates that at this location domestic heating and regional scale savannah and grassland fires are equally significant sources of eBC. Furthermore, MLR analyses supported the seasonality of eBC sources at Elandsfontein.

Although the source strengths of coal-fired power stations, pyro-metallurgical smelters and traffic emissions were lower than that of household combustion, as well as savannah and grassland fires, the first mentioned sources contribute year round, while the latter only contributed significantly in May to August, and June to September, respectively. Of the fresh industrial plumes, the highest eBC concentrations were associated with pyro-metallurgical smelters. This is a very significant finding, since coal-fired power stations and petrochemical operations have in the past been blamed for most of the pollution problems on the Mpumalanga Highveld (mainly due to the NO<sub>2</sub> hotspot over this area). Therefore, pyrometallurgical sources in this area need to be considered in greater detail in future studies.

Lastly, the calculated emission ratios of eBC and gaseous species that were presented could be used in future studies to assess the eBC emission inventories for industrial and domestic sources in South Africa.

## **5 Acknowledgements**

The European Union Framework Programme 6 (EU FP6), Eskom Holdings SOC Ltd and Sasol Technology R&D (Pty) Limited are acknowledged for funding. V Vakkari was a beneficiary of an AXA Research Fund postdoctoral grant. The financial support by the Saastamoinen Foundation is gratefully acknowledged for funding P Tiitta. The National Research Foundation (NRF) is acknowledged for providing research financial assistance (bursaries/scholarships) to P Maritz, AD Venter and K Jaars. Opinions expressed and conclusions arrived at are those of the authors and are not necessarily attributed to those of the NRF.

## 6 References

- Andreae, M.O., and Gelencser, A.: Black carbon or brown carbon? The nature of light absorbing carbonaceous aerosols. *Atmospheric Chemistry and Physics*, 6, 3131-3148, doi:10.5194/acp-6-3131-2006, 2006.
- Andrews, E., Massoli, P., Hallar, A.G., Sedlacek, A., Freedman, A., Ogren, J.A., and Sheridan, P.: Absorption closure-filter-based absorption instruments compared to extinction-scattering measurements. Poster presentation at the European Aerosol Conference, Grenada, Spain, September, 2012.
- Aurela, M., Beukes, J.P., Vakkari, V., Van Zyl, P.G., Teinilä, K., Saarikoski S. and Laakso L.: The composition of ambient and fresh biomass burning aerosols at a savannah site, *South African Journal of Science*, 112(5/6), Art. #2015-0223, 8 pages, doi:10.17159/sajs.2016/20150223, 2016.
- Awang, N.R., Ramli, N.Y., Ahmad, S., and Elbayoumi, M.: Multivariate methods to predict ground level ozone during daytime, nighttime, and critical conversion time in urban areas. *Atmospheric Pollution Research*, 6, 726-734. *Atmospheric Environment* 43, 3918-3924, doi:10.5094/APR.2015.081, 2015.
- Baldauf, R.W., Lane, D.D., Marotz, G.A., and Wiener, R.W.: Performance evaluation of the portable MiniVOL particulate matter sampler. *Atmospheric Environment*, 35, 6087-6091, doi:10.1016/S1352-2310(01)00403-4, 2001.
- Chow, J.C., Watson, J.G., Crow, D., Lowenthal, D.H., & Merrifield, T.: Comparison of IMPROVE and NIOSH carbon measurements. *Aerosol Science and Technology*, 34, 23-24, 2001.
- Beukes, J.P., Van Zyl, P.G. and Ras, M.: Treatment of Cr(VI)-containing wastes in the South African ferrochrome industry – a review of currently applied methods, *The Journal of The Southern African Institute of Mining and Metallurgy*, 112, 347-352, 2012.
- Beukes, J.P., Vakkari, V., Van Zyl, P.G., Venter, A.D., Josipovic, M., Jaars, K., Tiita, P., Siebert, S., Pienaar, J.J., Kulmala, M., and Laakso, L.: Welgegund: long-term land atmosphere measurement platform in South Africa. *iLeaps Newsletter*, 12, 24-25, 2013.
- Beukes, J.P., Vakkari, V., Van Zyl, P.G., Venter, A.D., Josipovic, M., Jaars, K., Tiitta, P., Kulmala, M., Worsnop, D., Pienaar, J.J., Virkkula, A. and Laakso, L.: Source region plume characterisation of the interior of South Africa as observed at Welgegund, *Clean Air Journal*, 23(1), 7-10, 2013.
- Bond, T., Streets, D.G., Yarber, K.F., Nelson, S.M., Woo, J-H. and Klimont, Z.: A technology-

1 based global inventory of black and organic carbon emissions from combustion. *Journal of*  
2 *Geophysical Research*, 109, doi:10.1029/2003JD003697, 2004.

3 Bond, T.C.: Can warming particles enter global climate discussions? *Environmental Research*  
4 *Letters* 2 (October-December 2007), 045030, doi:10.1088/1748-9326/2/4/045030, 2007.

5 Bond, T.C., Doherty, S.J., Fahey, D.W., Forster, P.M., Berntsen, T., DeAngelo, B.J., Flanner,  
6 M.G., Ghan, S., Kärcher, B., Koch, D., Kinne, S., Kondo, Y., Quinn, P., Sarofim, M.C.,  
7 Schultz, M.G., Schulz, M., Venkataraman, C., Zhang, H., Zhang, S., Bellouin, N.,  
8 Guttikunda, S.K., Hopke, P.K., Jacobson, M.Z., Kaiser, J.W., Klimont, Z., Lohmann, U.,  
9 Schwarz, J.P., Shindell, D., Storelvmo, T., Warren, S.G., and Zender, C.S.: Bounding the  
10 role of black carbon in the climate system: A scientific assessment. *Journal of Geophysical*  
11 *Research: Atmospheres*, 118, 5380-5552, doi:10.1002/jgrd.50171, 2013.

12 Cachier, H., Auglagnier, F., Sarda, R., Gautier, F., Masclet, P., Besombes, J.-L., Marchand, N.,  
13 Despiaud, S., Croci, D., Mallet, M., Laj, P., Marinoni, A., Deveau, P.-A., Roger, J.-C., Putaud,  
14 J.-P., Van Dingenen, R., Dell'Acqua, A., Viidanoja, J., Martins-Dos Santos, S., Liousse, C.,  
15 Cousin, F., Rosset, R. Gardrat, E., and Galy-Lacaux, C.: Aerosol studies during the  
16 ESCOMPTE experiment: An overview. *Atmospheric Research*, 74, 547-563,  
17 doi:10.1016/j.atmosres.2004.06.013, 2005.

18 Chow, J.C., Watson, J.G., Pritchett, L.C., Pierson, W.R., Frazier, C.A., and Purcell, R.G.: The  
19 DRI thermal/optical reflectance carbon analysis system: description, evaluation and  
20 applications in U.S. Air quality studies. *Atmospheric Environment*, 27, 1185-1201,  
21 doi:10.1016/0960-1686(93)90245-T, 1993.

22 Chow, J.C., Watson, J.G., Kuhns, H., Etyemezian, V., Lowenthal, D.H., Crow, D., Kohl, S.D.,  
23 Engelbrecht, J.P., and Green, M.C.: Source profiles for industrial, mobile, and area sources  
24 in the Big Bend Regional Aerosol Visibility and Observational study. *Chemosphere*, 54,  
25 185-208, doi:10.1016/j.chemosphere.2003.07.004, 2004.

26 Collett, K, Piketh, S. and Ross, K: An assessment of the atmospheric nitrogen budget on the  
27 South African Highveld, *South African Journal of Science*, 106,  
28 doi:10.4102/sajs.v106i5/6.220, 2010.

29 Conradie, E.H., Van Zyl, P.G., Pienaar, J.J., Beukes, J.P., Galy-Lacaux, C., Venter, A.D., and  
30 Mkhathshwa, G.V.: The chemical composition and fluxes of atmospheric wet deposition at  
31 four sites in South Africa, *Atmospheric Environment*, 146, 113-131,  
32 doi:10.1016/j.atmosenv.2016.07.033, 2016.

33 Cooke, W.F., and Wilson, J.N.: A global black carbon aerosol model. *Journal of Geophysical*

- Research 101D, 19395-19408, doi:10.1029/96JD00671, 1996.
- Draxler, R. R., and Hess, G. D.: Description of the HYSPLIT 4 Modelling System, NOAA Technical Memorandum ERL ARL-224, 2004.
- Environmental Analysis Facility (EAF). DRI Standard operating procedure. 86p. Laboratoire d'Aérodynamique – UMR 5560. <http://www.aero.obs-mip.fr/spip.php?article489>. Accessed 16 June 2016, 2008.
- Formenti, P., Elbert, W., Maenhaut, W., Haywood, J., Osborne, S., and Andreae, M.O.: Inorganic and carbonaceous aerosols during the Southern African Regional Science Initiative (SAFARI 2000) experiment: Chemical characteristics, physical properties, and emission data for smoke from African biomass burning. *Journal of Geophysical Research*, 108(D13), 8488, doi:10.1029/2002JD002408, 2003.
- Guillame, B., Liousse, C., Galy-Lacaux, C., Rosset, R., Gardrat, E., Cachier, H., Bessagnet, B., and Poisson, N.: Modeling exceptional high concentrations of carbonaceous aerosols observed at Pic du Midi in spring-summer 2003: Comparison with Sonnblick and Puy de Dôme. *Atmospheric Environment*, 42, 5140-5149, doi:10.1016/j.atmosenv.2008.02.024, 2008.
- Hansen, A.D.A., Rosen, H. and Novakov, T.: The Aethalometer: an instrument for real-time measurement of optical absorption by aerosol particles, *The Science of the Total Environment*, 36, 191-196, doi:10.1016/0048-9697(84)90265-1, 1984.
- Hirsikko, A., Vakkari, V., Tiitta, P., Manninen, H.E., Gagné, S., Laakso, H., Kulmala, M., Mirme, A., Mirme, S., Mabaso, D., Beukes, J.P. and Laakso, L.: Characterisation of sub-micron particle number concentrations and formation events in the western Bushveld Igneous Complex, South Africa, *Atmospheric Chemistry and Physics*, 12, 3951–3967, doi:10.5194/acp-12-3951-2012, 2012.
- Hyvärinen, A.-P., Vakkari, V., Laakso, L., Hooda, R.K., Sharma, V.P., Panwar, T.S., Beukes, J.P., Van Zyl, P.G., Josipovic, M., Garland, R.M., Andreae, M.O., Pöschl, U., and Petzold, A.: Correction for a measurement artifact of the Multi-Angle Absorption Photometer (MAAP) at high black carbon mass concentration levels. *Atmospheric Measurement Techniques*, 6, 81-90, doi:10.5194/amt-6-81-2013, 2013.
- HYSPLIT User's Guide-Version 4. Last revised: April 2013. [http://www.arl.noaa.gov/documents/reports/hysplit\\_user\\_guide.pdf](http://www.arl.noaa.gov/documents/reports/hysplit_user_guide.pdf). Accessed 13 February 2014.
- Galy-Lacaux, C., Al Ourabi, H., Lacaux, J.-P., Pont, V., Galloway, J., Mphepya, J., Pienaar, K.,

- 1     Sigha, L., and Yoboué, V.: Dry and wet atmospheric nitrogen deposition in Africa. IGAC  
2     Newsletter, January 2003, Issue no. 27, 6-11, 2003.
- 3     Garstang, M., Tyson, M., Swap, R., Edwards, M., K<sup>o</sup>allberg, P., and Lindesay, J. A.: Horizontal  
4     and vertical transport of air over southern Africa, *Journal of Geophysical Research*, 101,  
5     23721-23736, doi:10.1029/95JD00844, 1996.
- 6     IPCC: Changes in atmospheric constituents and in radiative forcing, in *climate change 2007:*  
7     *The Physical Science Basis. Contribution of Working Group I to the Fourth Assessment*  
8     *Report of the Intergovernmental Panel on Climate Change*, 129, 132; available at  
9     <http://www.ipcc.ch/ipccreports/ar4-wg1.htm>, accessed: 18 November 2011, 2007.
- 10    IPCC: Summary for Policymakers. In: *Climate Change 2013: The Physical Science Basis.*  
11    *Contribution of Working Group I to the Fifth Assessment Report of the Intergovernmental*  
12    *Panel on Climate Change* [Stocker, T.F., D. Qin, G.K. Plattner, M. Tignor, S.K. Allen, J.  
13    Boschung, A. Nauels, Y. Xia, V. Bex and P.M. Midgley (eds.)]. Cambridge University Press,  
14    Cambridge, United Kingdom and New York, NY, USA.
- 15    Jaars, K., Beukes, J.P., Van Zyl, P.G., Venter, A.D., Josipovic, M., Pienaar, J.J., Vakkari, V.,  
16    Aaltonen, H., Laakso, H., Kulmala, M., Tiitta, P., Guenther, A., Hellén, H., Laakso, L., and  
17    Hakola, H.: Ambient aromatic hydrocarbon measurements at Welgegund, South Africa.  
18    *Atmospheric Chemistry and Physics*, 14, 7075-7089, doi:10.5194/acpd-14-7075-2014,  
19    2014.
- 20    Jacobson, M., 2004. Climate response of fossil fuel and biofuel soot, accounting for soot's  
21    feedback to snow and sea ice albedo and emissivity, 109 *Journal of Geophysical Research:*  
22    *Atmospheres*, 109, D21201, doi:10.1029/2004JD004945, 2004.
- 23    Kanakidou, M., Seinfeld, J.H., Pandis, S.N., Barnes, I., Dentener, F.J., Facchini, M.C., Van  
24    Dingenen, R., Ervens, B., Nenes, A., Nielson, C.J., Swietlicki, E., Putaud, J.P., Balkanski,  
25    Y., Fuzzi, S., Horth, J., Moortgat, G.K., Winterhalter, R., Myhre, C.E.L., Tsigaridis, K.,  
26    Vignati, E., Stephanou, E.G., and Wilson, J.: Organic aerosol and global climate modelling:  
27    a review. *Atmospheric chemistry and Physics*, 5, 1053-1123, doi:10.1029/2005-5-  
28    1053, 2005.
- 29    Korhonen, K., Giannakaki, E., Mielonen, T., Pfüller, A., Laakso, L., Vakkari, V., Baars, H.,  
30    Engelmann, R., Beukes, J. P., Van Zyl, P. G., Ramandh, A., Ntsangwane, L., Josipovic, M.,  
31    Tiitta, P., Fourie, G., Ngwana, I., Chiloane, K., and Komppula, M.: Atmospheric boundary  
32    layer top height in South Africa: measurements with lidar and radiosonde compared to three  
33    atmospheric models, *Atmospheric Chemistry and Physics*, 14, 4263-4278, doi:10.5194/acp-

14-4263-2014, 2014.

Kuik, F., Lauer, A., Beukes, J.P., Van Zyl, P.G., Josipovic, M., Vakkari, V., Laakso, L. and Feig, G.T.: The anthropogenic contribution to atmospheric black carbon concentrations in southern Africa: a WRF-Chem modeling study, *Atmospheric Chemistry and Physics*, 15, 8809–8830, doi:10.5194/acp-15-8809-2015, 2015.

Kulmala, M., Asmi, A., Lappalainen, H., Carslaw, K. S., Pöschl, U., Baltensperger, U., Hov, Ø., Brenguier, J.-L., Pandis, S. N., Facchini, M. C., Hansson, H.-C., Wiedensohler, A., and O'Dowd, C.D.: Introduction: European Integrated Project on Aerosol Cloud Climate and Air Quality interactions (EUCAARI). Integrating aerosol research from nano to global scales, *Atmospheric Chemistry and Physics* 9, 2825-2841, 2009.

Laakso, L., Vakkari, V., Virkkula, A., Laakso, H., Backman, J., Kulmala, M., Beukes, J.P., van Zyl, P.G., Tiitta, P., Josipovic, M., Pienaar, J.J., Chiloane, K., Gilardoni, S., Vignati, E., Wiedensohler, A., Tuch, T., Birmili, W., Piketh, S., Collett, K., Fourie, G.D., Komppula, M., Lihavainen, H., de Leeuw, G., and Kerminen, V.-M.: South African EUCAARI measurements: seasonal variation of trace gases and aerosol optical properties. *Atmospheric Chemistry and Physics*, 12, 1847-1864, doi:10.5194/acp-12-1847-2012, 2012.

Lioussé, C., Penner, J.E., Chuang, C., Walton, J.J., Eddleman, H., and Cachier, H.: A global three-dimensional model study of carbonaceous aerosols. *Journal of Geophysical Research*, 105, 26871-26890, 1996.

Lourens, A.S., Beukes, J.P., and Van Zyl, P.G.: Spatial and temporal assessment of gaseous pollutants in the Highveld of South Africa. *South African Journal of Science*, 107(1/2), Art. #269, 8 pages, doi: 10.4102/sajs.v107i1/2.269, 2011.

Lourens, A.S.M., Butler, T.M., Beukes, J.P., Van Zyl, P.G., Fourie, G.D., Lawrence, M.G.: Investigating atmospheric photochemistry in the Johannesburg-Pretoria megacity using a box model, *South African Journal of Science*, 112(1/2), Art. #2015-0169, 11 pages, doi:10.17159/sajs.2016/2015-0169, 2016.

Mafusire, G., Annegarn, H.J., Vakkari, V., Beukes, J.P., Josipovic, M., Van Zyl, P.G. and Laakso, L.: Submicrometer aerosols and excess CO as tracers for biomass burning air mass transport over southern Africa, *Journal of Geophysical Research – Atmospheres*, 121, 10262-10282, doi:10.1002/2015JD023965, 2016.

Martins, J.J., Dhammapala, R.S., Lachmann, G., Galy-Lacaux, C., & Pienaar, J.J.: Long-term measurements of sulphur dioxide, nitrogen dioxide, ammonia, nitric acid and ozone in southern Africa using passive samplers. *South African Journal of Science*, 103, 336-342.

2007.

Martins, J.J.: Concentrations and deposition of atmospheric species at regional sites in southern Africa. MSc thesis NWU Potchefstroom, 224p. 2009.

Masiello, C.A.: New directions in black carbon organic geochemistry. *Marine Chemistry* 92, 201-213, doi:10.1016/j.marchem.2004.06.043, 2004.

MODIS: Obtaining and processing MODIS data.  
[http://www.yale.edu/ceo/Documentation/MODIS\\_data.pdf](http://www.yale.edu/ceo/Documentation/MODIS_data.pdf).

Mokdad, Ali H.: Actual Causes of Death in the United States, 2000. *Journal of American Medical Association*, 291 (10), 1238-1245, 2004.

Mphopya, J.N., Pienaar, J.J., Galy-Lacaux, C., Held, G., and Turner, C.R.: Precipitation Chemistry in Semi-Arid Areas of Southern Africa: A Case Study of a Rural and an Industrial Site. *Journal of Atmospheric Chemistry*, 47, 1-24, doi:10.1023/B:JOCH.0000012240.09119.c4, 2004.

Maritz, P., Beukes, J.P., Van Zyl, P.G. Conradie, E.H., Liousse, C., Galy-Lacau, C., Castéra, P., Ramandh, A., Mkhathshwa, G., Venter, A.D. and Pienaar, J.J.: Spatial and temporal assessment of organic and black carbon at four sites in the interior of South Africa, *Clean Air Journal*, 25(1), 20-33, doi:10.17159/2410-972X/2015/v25n1a1, 2015.

Petzold, A., and Schönlinner, M.: Multi-angle absorption photometry: a new method for the measurement of aerosol light absorption and atmospheric black carbon. *Journal of Aerosol Science* 35, 421-441, doi:10.1016/j.jaerosci.2003.09.005, 2004.

Petzold, A., Ogren, J. A., Fiebig, M., Laj, P., Li, S.-M., Baltensperger, U., Holzer-Popp, T., Kinne, S., Pappalardo, G., Sugimoto, N., Wehrli, C., Wiedensohler, A., and Zhang, X.-Y.: Recommendations for reporting “black carbon” measurements, *Atmospheric Chemistry and Physics*, 13, 8365–8379, doi:10.5194/acp-13-8365-2013, 2013.

Pope, C.A., Burnett, R.T., Thun, M.J., Calle, E.E., Krewski, D., Ito, K., and Thurston, G.D.: Lung cancer, cardiopulmonary mortality, and long-term exposure to fine particulate air pollution. *Journal of the American Medical Association*, 287 (9), 1132–1141, 2002.

Pöschl, U.: *Atmospheric Aerosols: Composition, Transformation, Climate and Health Effects. Atmospheric Chemistry: Reviews. Angewandte Chemie International Edition*, 44, 7520-7540, doi:10.1002/anie.200501122, 2005.

Putaud, J.-P., Raes, F., Van Dingenen, R., Brüggemann, E., Facchini, M.-C., Decesari, S., Fuzzi, S., Gehrig, R., Hüglin, C., Laj, P., Lorbeer, G., Maenhaut, W., Mihalopoulos, N., Müller, K., Querol, X., Rodriguez, S., Schneider, J., Spindler, G., ten Brink, H., Tørseth, K., and



- 1 Wiedensohler, A.: A European aerosol phenomenology e 2: chemical characteristics of  
2 particulate matter at kerbside, urban, rural and background sites in Europe. *Atmospheric*  
3 *Environment*, 38, 2579-2595, doi:10.1016/j.atmosenv.2004.01.041, 2004.
- 4 Ramanathan, V., and Carmichael, G.: Global and regional climate changes due to black carbon.  
5 *Nature Geoscience* 1, 221-227, doi:10.1038/ngeo156, 2008.
- 6 Roy, D.P., Boschetti, L., Justice, C.O., and Ju, J.: The collection 5 MODIS burned area product:  
7 Global evaluation by comparison with the MODIS active fire product. *Remote Sensing of*  
8 *Environment*, 112, 3690-3707p. doi:10.1016/j.rse.2008.05.013, 2008.
- 9 Saha A., and Despiou S.: Seasonal and diurnal variations of black carbon aerosols over a  
10 Mediterranean coastal zone. *Atmospheric Research*, 92, 27-41,  
11 doi:10.1016/j.atmosres.2008.07.007, 2009
- 12 Scholes, R.J., Ward, D.E. and Justice, C.O.: Emissions of trace gases and aerosol particles due  
13 to vegetation burning in southern hemisphere Africa. *Journal of Geophysical Research*,  
14 101(D19): 23,677-23,682, 1996.
- 15 Sehloho, R.M.: An assessment of atmospheric organic and black carbon at Welgegend. PhD  
16 thesis in preparation, [North-West University, Potchefstroom Campus, South Africa](#), 2017.
- 17 Shindell, D.T., Levy II, H., Schwarzkopf, M.D., Horowitz, L.W., Lamarque, J.-F., and  
18 Faluvegi, G.: Multimodel projections of climate change from short-lived emissions due to  
19 human activities. *Journal of Geophysical Research – Atmospheres*, 113, D11109.  
20 doi:10.1029/2007JD009152, 2008.
- 21 Stohl, A.: Computation, accuracy and application of trajectories – a review and bibliography.  
22 *Atmospheric Environment*, 32(6), 947-966, doi: 10.1016/S1352-2310(97)00457-3, 1998.
- 23 Swap, R.J., Aranibar, J.N., Dowty, P.R., Gilhooly (III), W.P., and Macko, S.A.: Natural  
24 abundance of  $^{13}\text{C}$  and  $^{15}\text{N}$  in  $\text{C}_3$  and  $\text{C}_4$  vegetation of southern Africa: patterns and  
25 implications. *Global Change Biology*, 10, 350-358, doi:10.1046/j.1529-8817.2003.00702.x,  
26 2004.
- 27 Swap, R.J., Annegarn, H.J., Suttles, J.T., King, M.D., Platnick, S., Privette, J.L., and Scholes  
28 R.J.: Africa burning: A thematic analysis of the Southern African Regional Science Initiative  
29 (SAFARI 2000), *Journal of Geophysical Research*, 108, 8465, doi:10.1029/2003JD003747,  
30 2003.
- 31 Tummon, F., Solmon, F., Liousse, C., and Tadross, M.: Simulation of the direct and semidirect  
32 aerosol effects on the southern Africa regional climate during the biomass burning season.  
33 *Journal of Geophysical Research D: Atmospheres*, 115(19). Art. no. D19206,

doi:10.1029/2009JD013738, 2010.

Tiitta, P., Vakkari, V., Croteau, P., Beukes, J.P., Van Zyl, P.G., Josipovic, M., Venter, A.D., Jaars, K., Pienaar, J.J., Ng, N.L., Canagaratna, M.R., Jayne, J.T., Kerminen, V.-M., Kokkola, H., Kulmala, M., Laaksonen, A., Worsnop, D.R., and Laakso, L.: Chemical composition, main sources and temporal variability of PM<sub>1</sub> aerosols in southern African grassland. *Atmospheric Chemistry and Physics*, 14, 1909–1927, doi:10.5194/acp-14-1909-2014, 2014.

Venter, A.D., Vakkari, V., Beukes, J.P., Van Zyl, P.G., Laakso, H., Mabaso, D., Tiitta, P., Josipovic, M., Kulmala, M., Pienaar, J.J., and Laakso, L. An air quality assessment in the industrialised western Bushveld Igneous Complex, South Africa. *South African Journal of Science*, 108(9/10), Art. #1059, 10 pages, doi:10.4102/sajs.v108i9/10.1059, 2012

Venter, A.D., Beukes, J.P., van Zyl, P.G., Brunke, E.G., Labuschagne, C., Slemr, F., Ebinghaus, R., and Kock, H.: Statistical exploration of gaseous elemental mercury (GEM) measured at Cape Point from 2007 to 2011. *Atmospheric Chemistry and Physics*, 15, 10271-10280, doi:10.5194/acp-15-10271-2015, 2015.

Venter, A.D., Beukes, J.P., Van Zyl, P.G., Josipovic, M., Jaars, K. and Vakkari, V.: Regional atmospheric Cr(VI) pollution from the Bushveld Complex, South Africa. *Atmospheric Pollution Research*, 7, 762-767, doi:10.1016/j.apr.2016.03.009, 2016.

Viidanoja, J., Sillanpää, M., Laakia, J., Kerminen, V.-M., Hillamo, R., Aarnio, P., and Koskentalo, T.: Organic and black carbon in PM<sub>2.5</sub> and PM<sub>10</sub>: 1 year of data from an urban site in Helsinki, Finland. *Atmospheric Environment*, 36, 3183-3193, doi:10.1016/S1352-2310(02)00205-4, 2002.

Watson J.G., Chow, J.C., and Chen, L.-W.A.: Summary of Organic and Elemental Carbon/Black Carbon Analysis Methods and Intercomparisons. *Aerosol and Air Quality Research*, 5, 65-102, 2005.

Wolf, E.W., and Cachier, H.: Concentrations and seasonal cycle of black carbon in aerosol at a coastal Antarctic station. *Journal of Geophysical Research*, 103D, 11033-11041, 1998.

Yttri, K.E., Aas, W., Bjerke, A., Cape, J.N., Cavalli, F., Ceburnis, D., Dye, C., Emblico, L., Facchini, M.C., Forster, C., Hanssen, J.E., Hansson, H.C., Jennings, S.G., Maenhaut, W., and Putaud, J.P., Torseth, K.: Elemental and organic carbon in PM<sub>10</sub>: a one year measurement campaign within the European Monitoring and Evaluation Program EMEP. *Atmospheric Chemistry and Physics*, 7, 5711-5725, 2007.

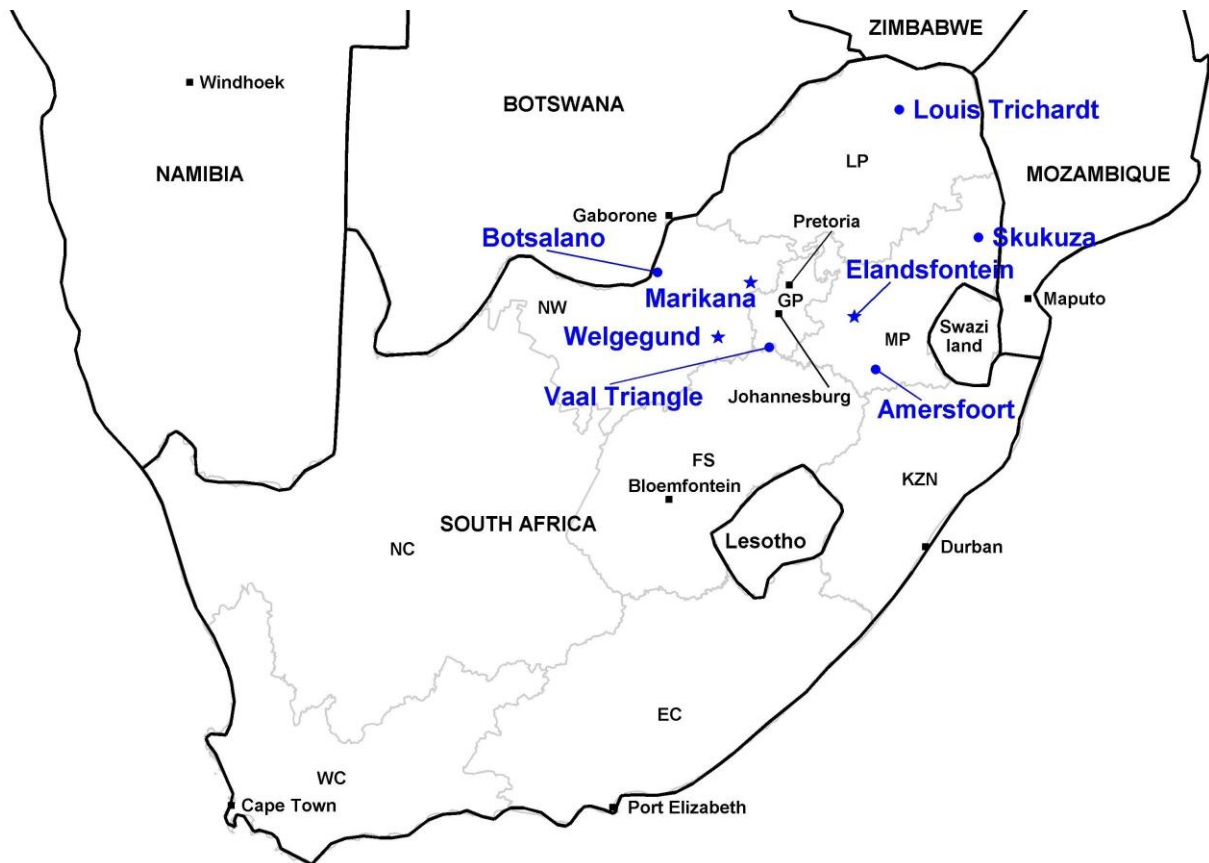


Figure 1. The sites (Elandsfontein, Welgegend and Marikana) where continuous high resolution data were gathered are indicated with blue stars, while the sites (Louis Trichardt, Skukuza, Vaal Triangle, Amersfoort and Botsalano) where filters were gathered and analysed off-line are indicated with blue dots. Neighbouring countries, some major cities and South African provincial borders are also indicated for additional regional contextualisation (Provinces: WC = Western Cape; EC = Eastern Cape; NC = Northern Cape; FS = Free State; KZN = KwaZulu-Natal; NW = North West; GP = Gauteng; MP = Mpumalanga and LP = Limpopo).

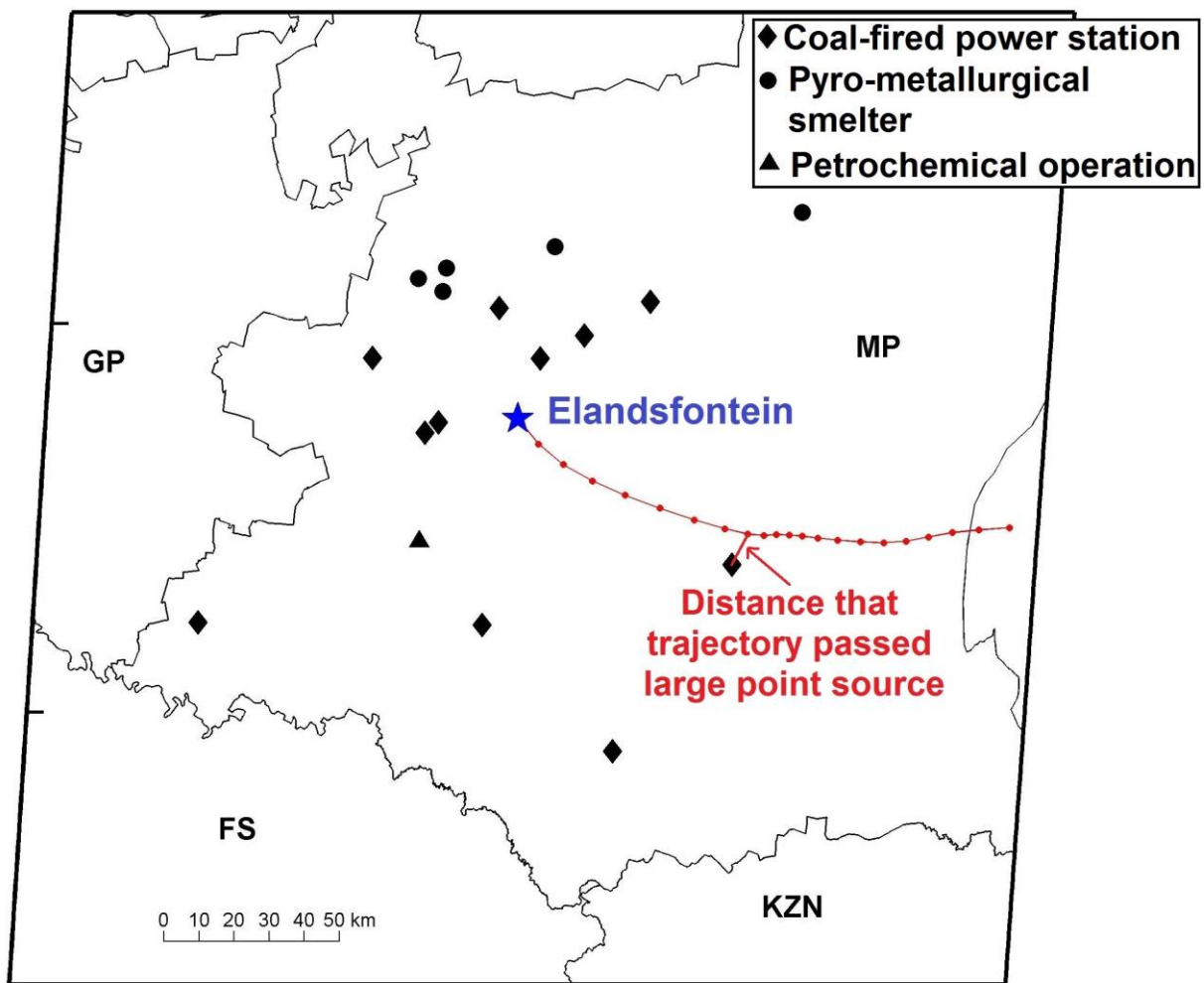


Figure 2. Example to illustrate the method applied to determine the shortest distance that each 24-hour back trajectory passed large point sources and/or in- or semi-formal settlements. (Provinces: FS = Free State; KZN = KwaZulu-Natal; NW = North West; GP = Gauteng and MP = Mpumalanga)

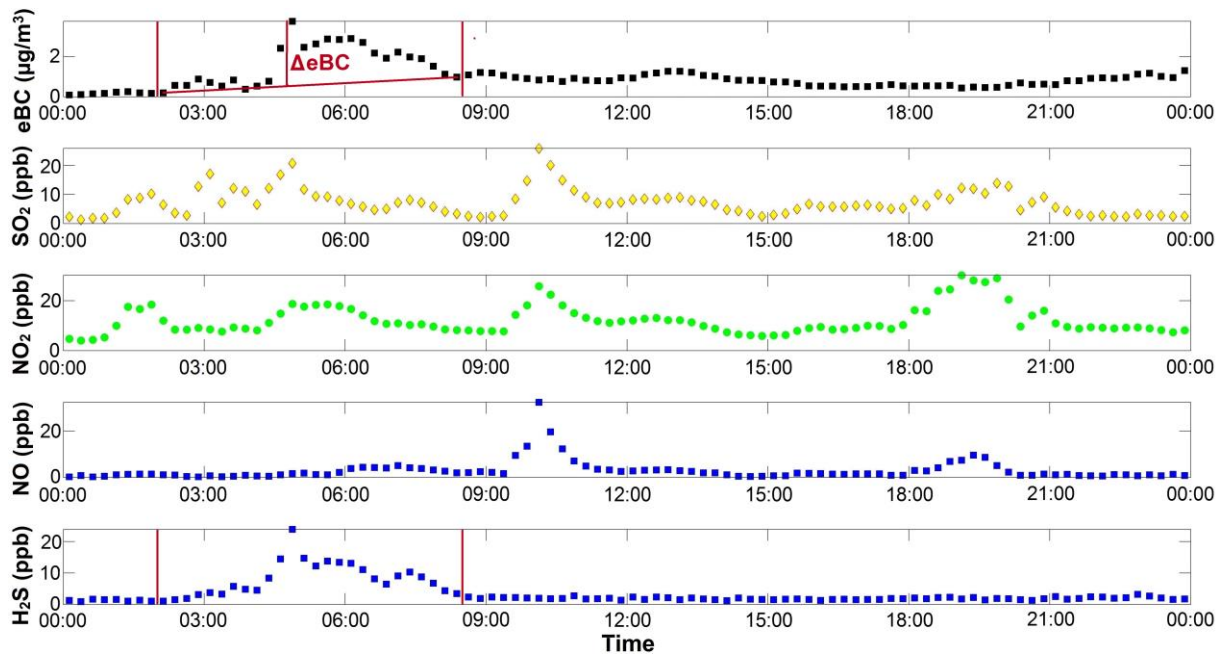


Figure 3. Example to illustrate how species were correlated with eBC in order to separate sources from one another. The excess eBC ( $\Delta$  eBC), defined as the eBC concentration above the baseline for this example, is also indicated in the top pane.

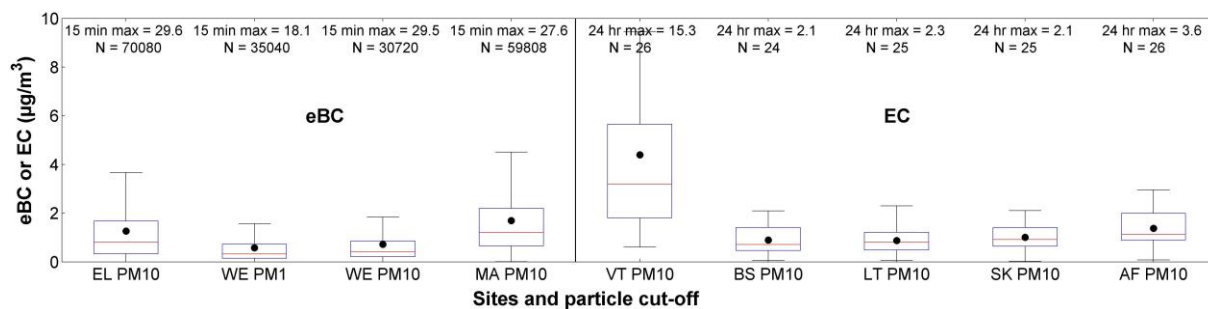


Figure 4. Box and whisker plot indicating statistical eBC mass concentrations at the Elandsfontein (EL), Welgegund (WE) and Marikana (MA) sites, as well as EC mass concentrations at the Vaal Triangle (VT), Botsalano (BS), Louis Trichardt (LT), Skukuza (SK) and Amersfoort (AF) sites. The red line of each box indicates the median, the black dot the mean, the top and bottom edges of the box the 25<sup>th</sup> and 75<sup>th</sup> percentiles and the whiskers  $\pm 2.7\sigma$  (99.3% coverage if the data has a normal distribution). The 15-minute and 24-hour maximum mass concentration values measured at the sites with continuous and off-line analyses, respectively, as well as the number of measurements (N) are indicated.

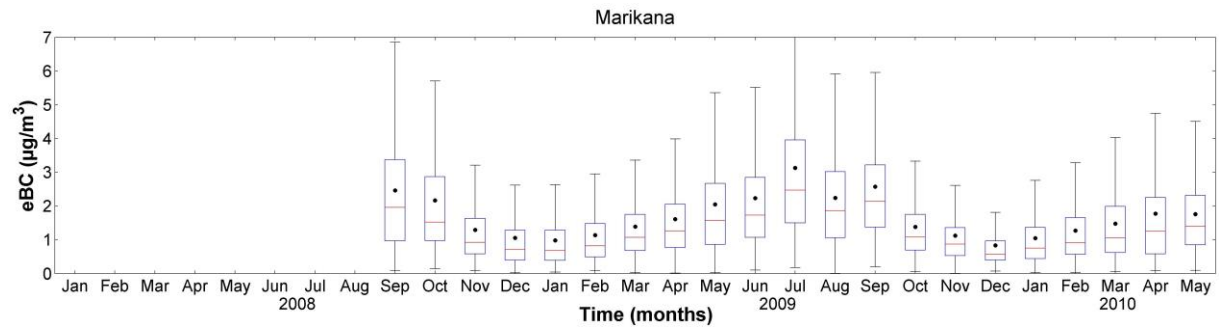
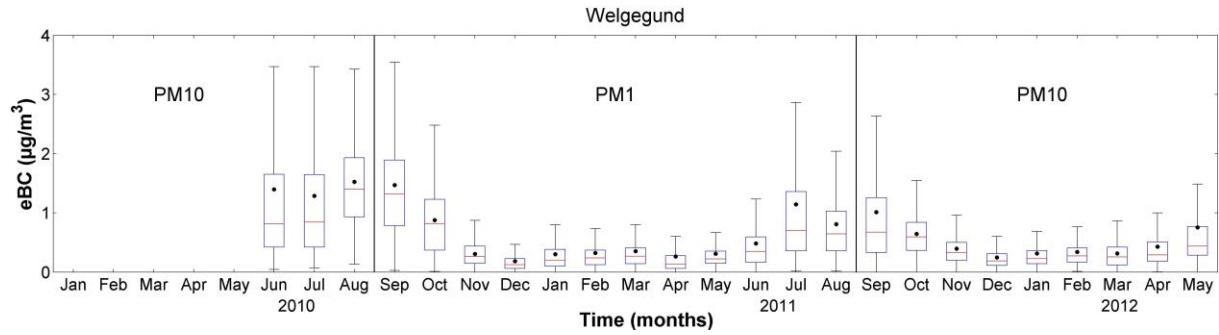
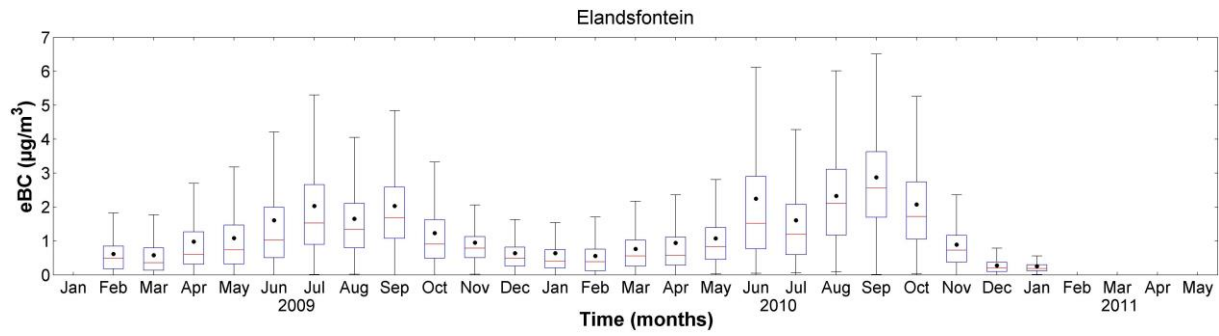


Figure 5. Monthly statistical distribution of eBC concentrations at the three sites where continuous measurement data were gathered, i.e. Elandsfontein, Welgegund and Marikana. PM<sub>10</sub> inlets were used at Elandsfontein and Marikana, while measurements at Welgegund were conducted with either a PM<sub>1</sub> or PM<sub>10</sub> inlet. The red line of each box is the median, the black dots indicate the mean, the top and bottom edges of the box are the 25<sup>th</sup> and 75<sup>th</sup> percentiles and the whiskers  $\pm 2.7\sigma$  (99.3% coverage if the data has a normal distribution).

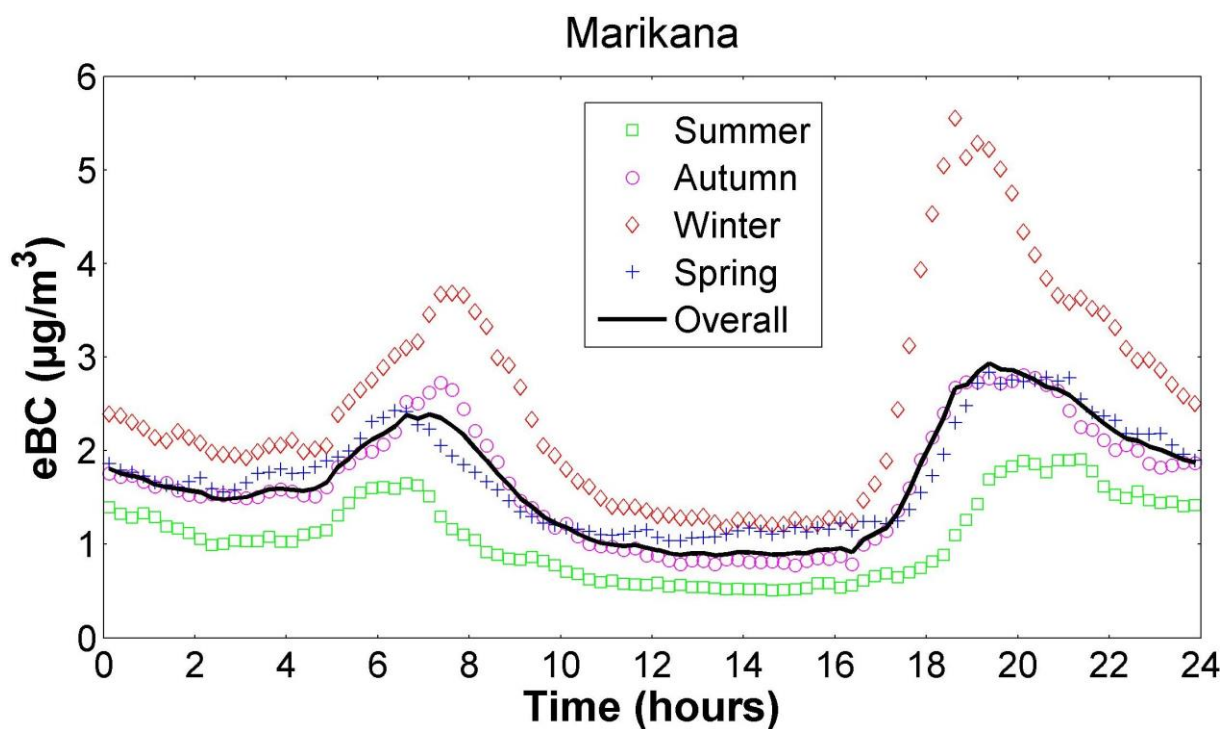
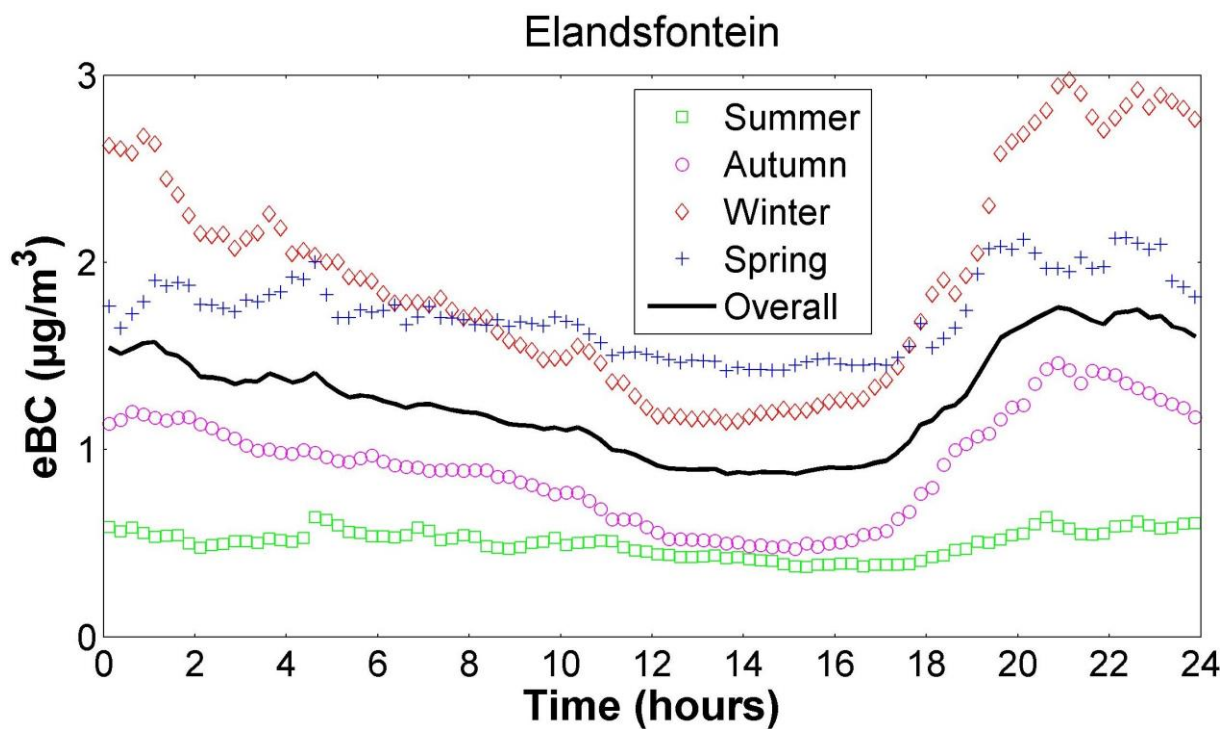


Figure 6. Overall (all the data) and seasonal (each season separately) average eBC diurnal patterns observed for Elandsfontein, Welgegund and Marikana. Summer: DJF, Autumn: MAM, Winter: JJA and Spring: SON.



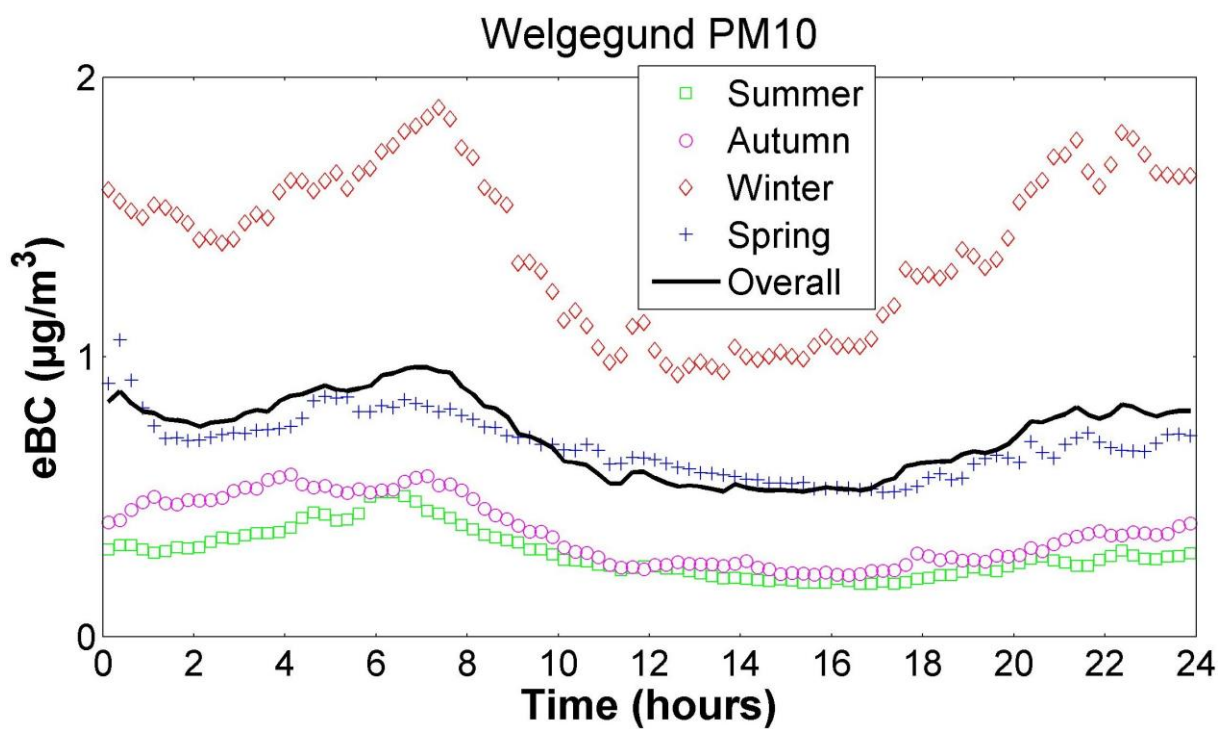
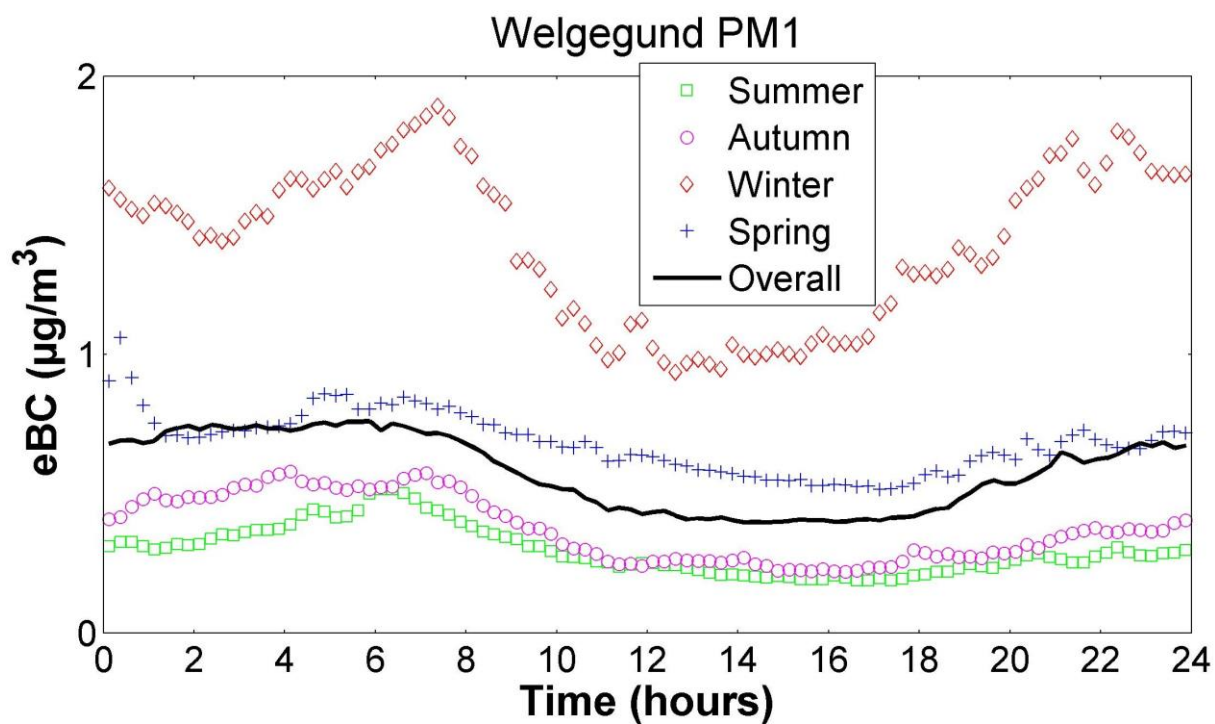


Figure 6 (continue). Overall (all the data) and seasonal (each season separately) average eBC diurnal patterns observed for Elandsfontein, Welgegund and Marikana. Summer: DJF, Autumn: MAM, Winter: JJA and Spring: SON.

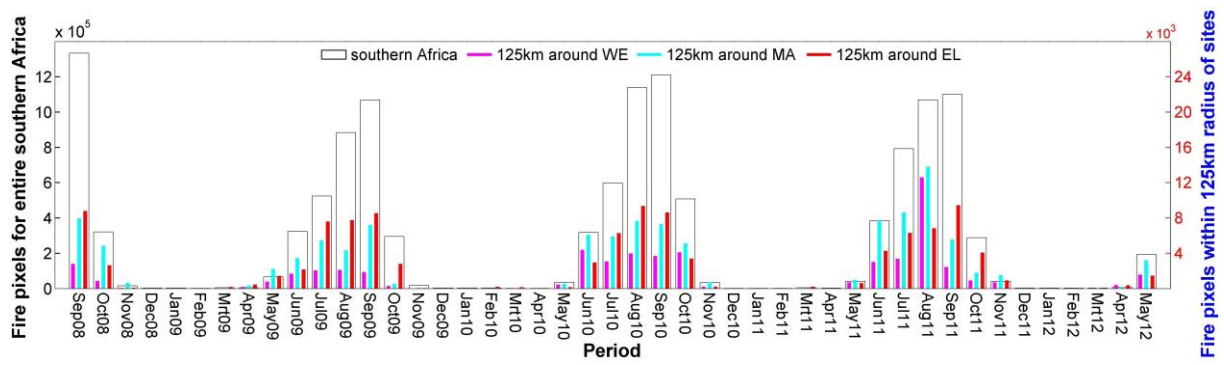


Figure 7. Fire pixels within the entire southern Africa (10-35°S and 10-41°E) indicated on the primary y-axis, as well as fires pixels within a radius of 125 km around Elandsfontein (EL), Marikana (MA) and Welgegund (WE) measurement sites indicated on the secondary y-axis, as determined from MODIS collection 5 burned area product (Roy et al., 2008).

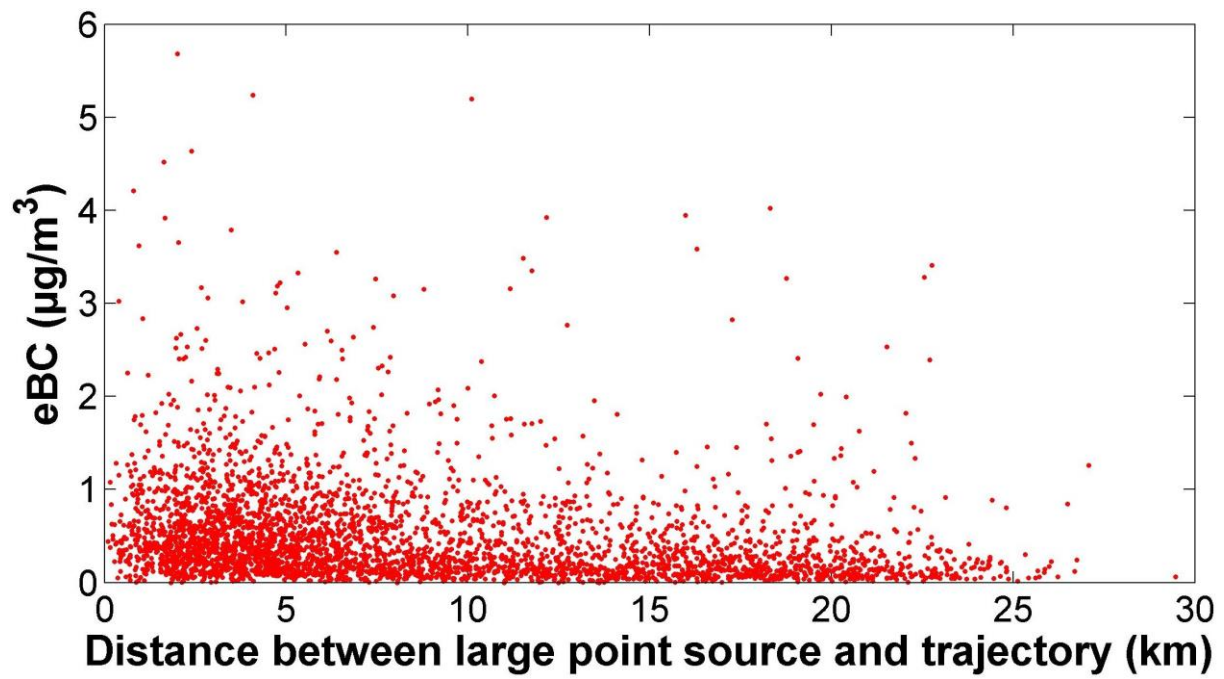
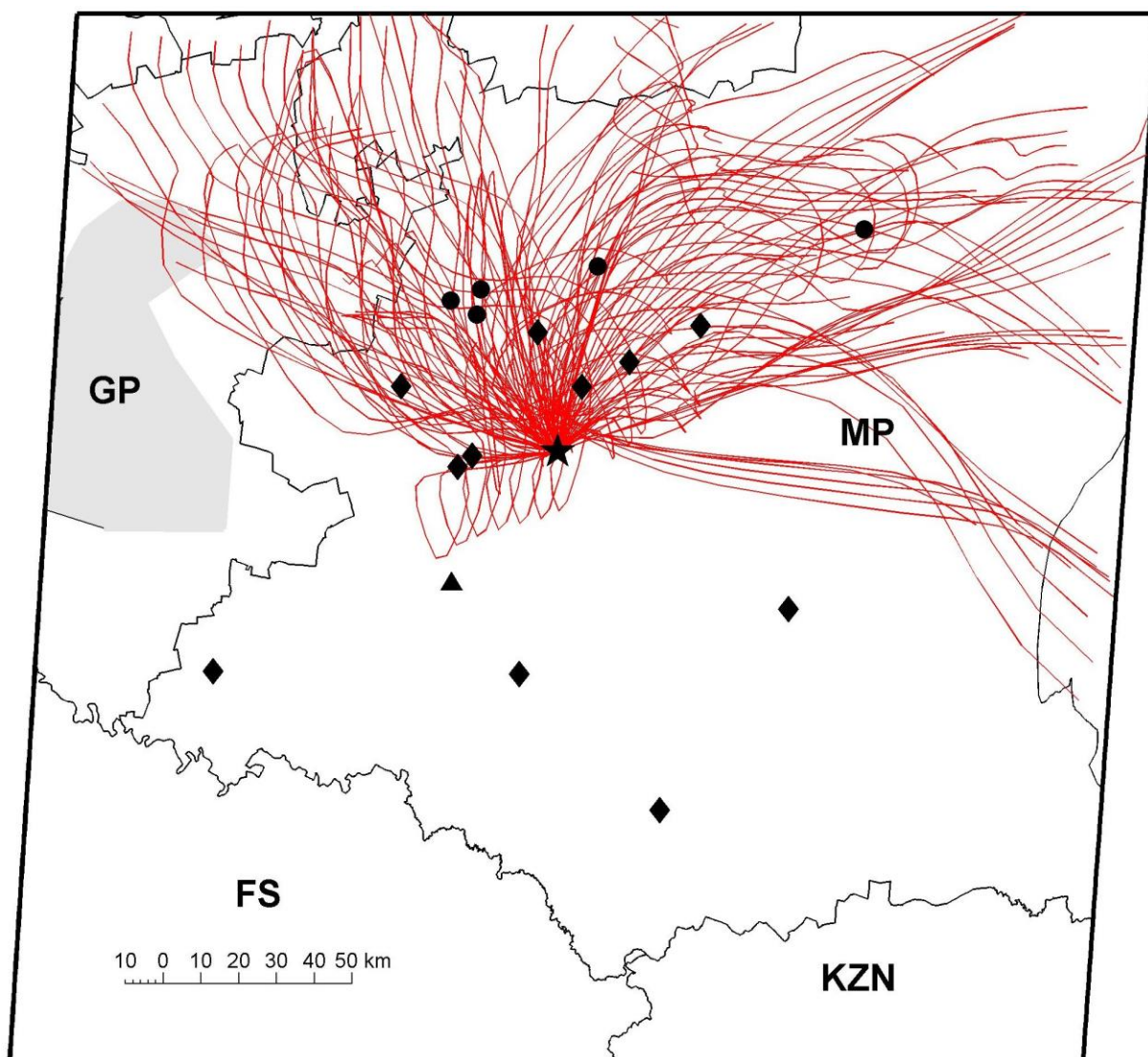
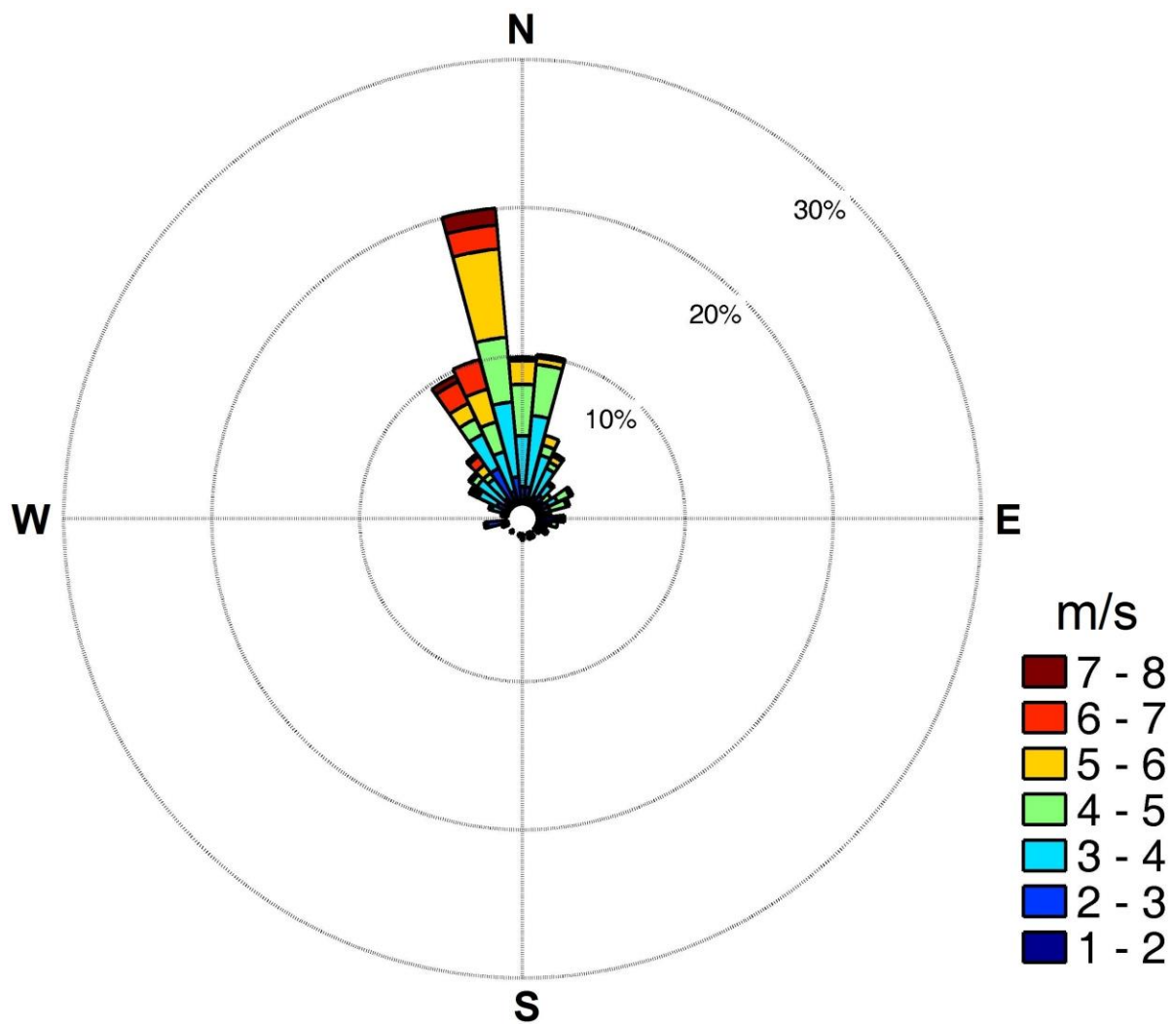


Figure 8. Hourly average eBC concentrations plotted against the shortest distances that hourly arriving back trajectories passed large point sources during the summer months, i.e. December to February, at Elandsfontein.



(a)

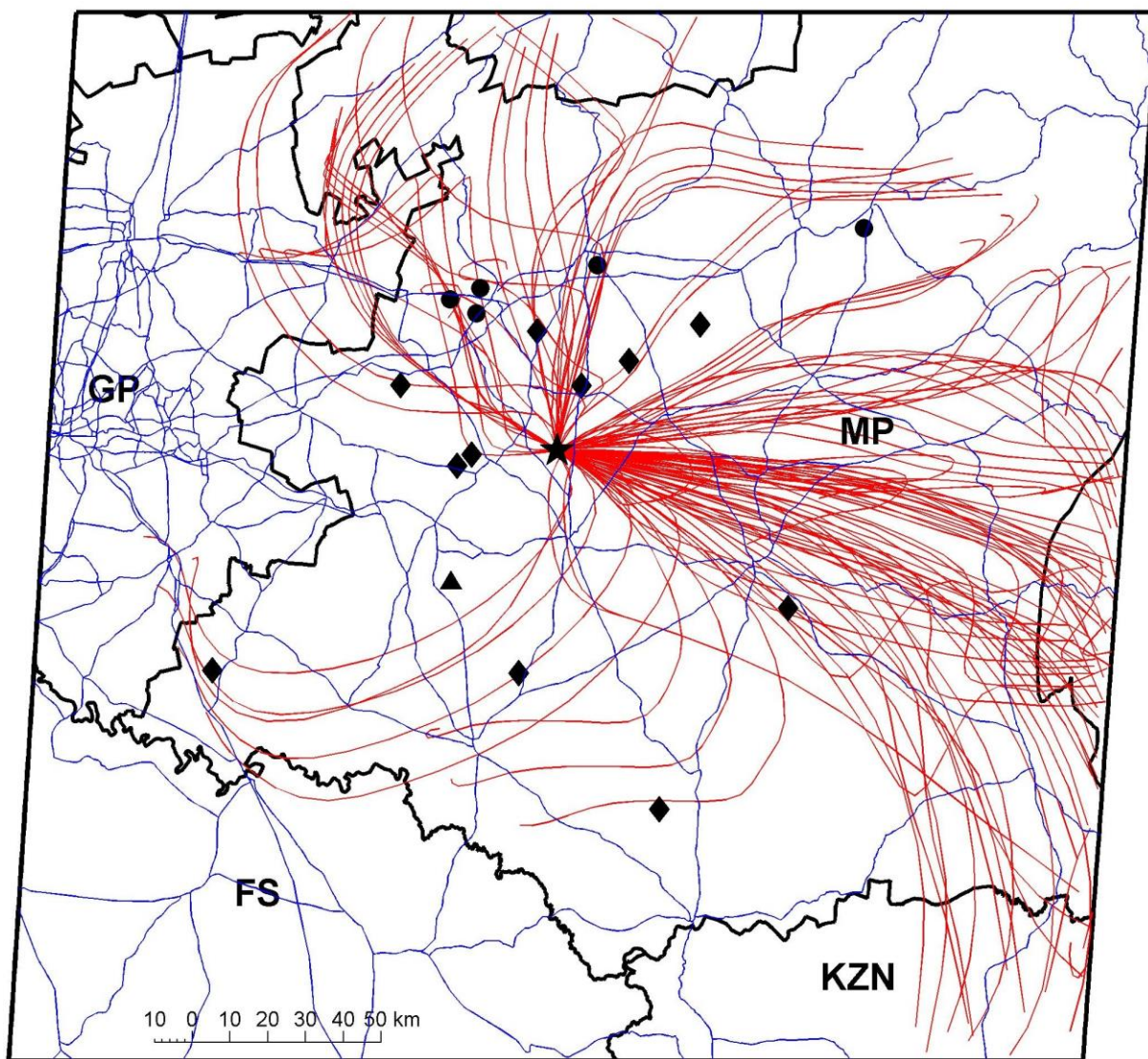
Figure 9. (a) All 24-hour back trajectories associated with peaks characterised by coincidental increases in eBC and  $\text{H}_2\text{S}$  during December to February. The Elandsfontein site is indicated by the black star. The black dots indicate pyro-metallurgical smelters and char plants, the black diamonds coal-fired power plants and the black triangle a large petrochemical operation. (b) Wind rose showing the prevailing wind direction during periods when eBC plumes that coincided with  $\text{H}_2\text{S}$  plumes were observed.



(b)

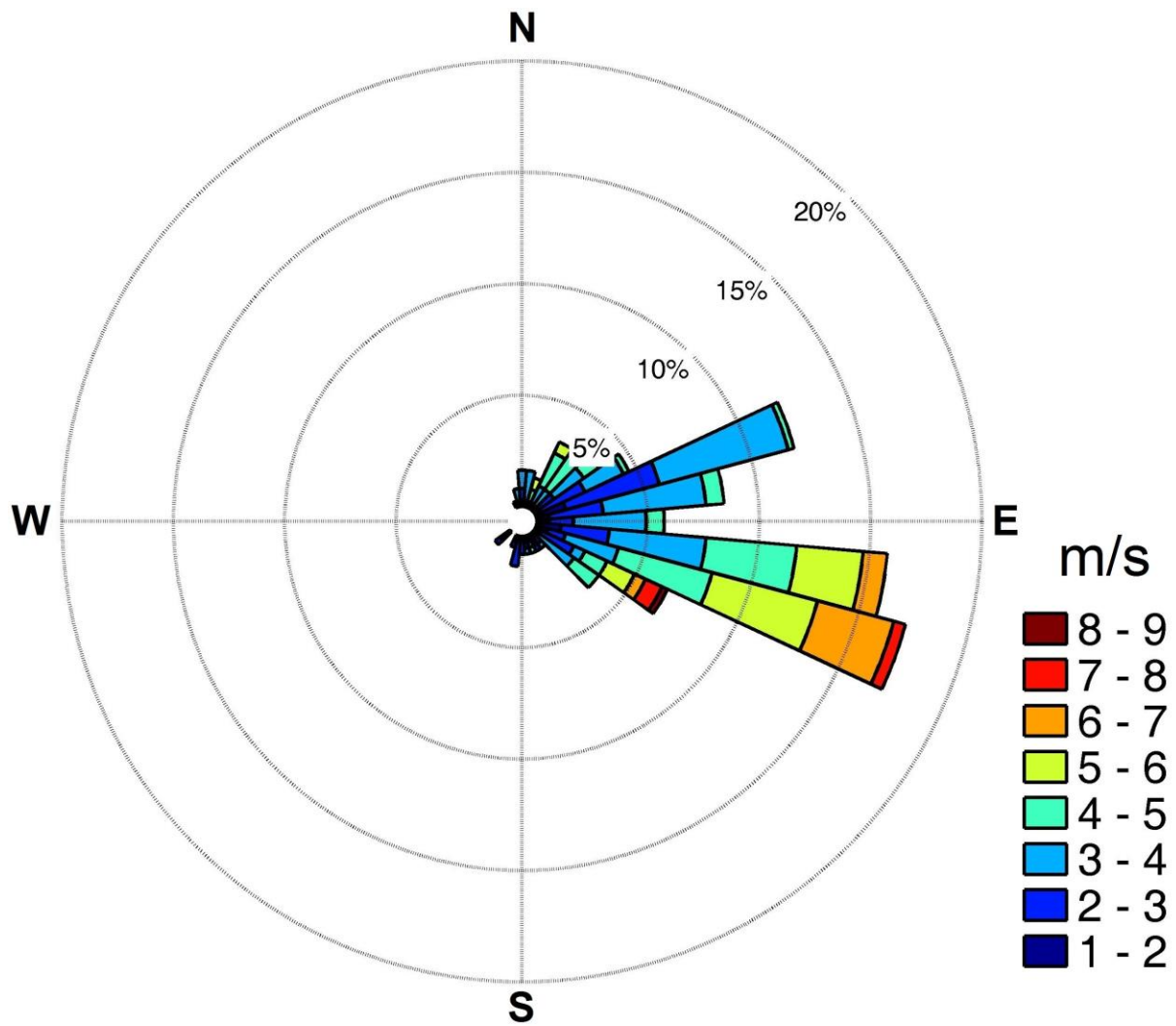
Figure 9 (continue). (a) All 24-hour back trajectories associated with peaks characterised by coincidental increases in eBC and H<sub>2</sub>S during December to February. The Elandsfontein site is indicated by the black star. The black dots indicate pyrometallurgical smelters and char plants, the black diamonds coal-fired power plants and the black triangle a large petrochemical operation. (b) Wind rose showing the prevailing wind direction during periods when eBC plumes that coincided with H<sub>2</sub>S plumes were observed.





(a)

Figure 10. (a) All 24-hour back trajectories associated with peaks characterised by coincidental increases in eBC and  $\text{NO}_2$  during December to February. The Elandsfontein site is indicated by the black star. The black dots indicate pyro-metallurgical smelters and char plants, the black diamonds indicate coal-fired power plants and the black triangle a large petrochemical operation. Roads are indicated with blue lines. (b) Wind rose showing the prevailing wind direction during periods when eBC plumes that coincided with  $\text{NO}_2$  plumes were observed.



(b)

Figure 10 (continue). (a) All 24-hour back trajectories associated with peaks characterised by coincidental increases in eBC and NO<sub>2</sub> during December to February. The Elandsfontein site is indicated by the black star. The black dots indicate pyrometallurgical smelters and char plants, the black diamonds indicate coal-fired power plants and the black triangle a large petrochemical operation. Roads are indicated with blue lines. (b) Wind rose showing the prevailing wind direction during periods when eBC plumes that coincided with NO<sub>2</sub> plumes were observed.

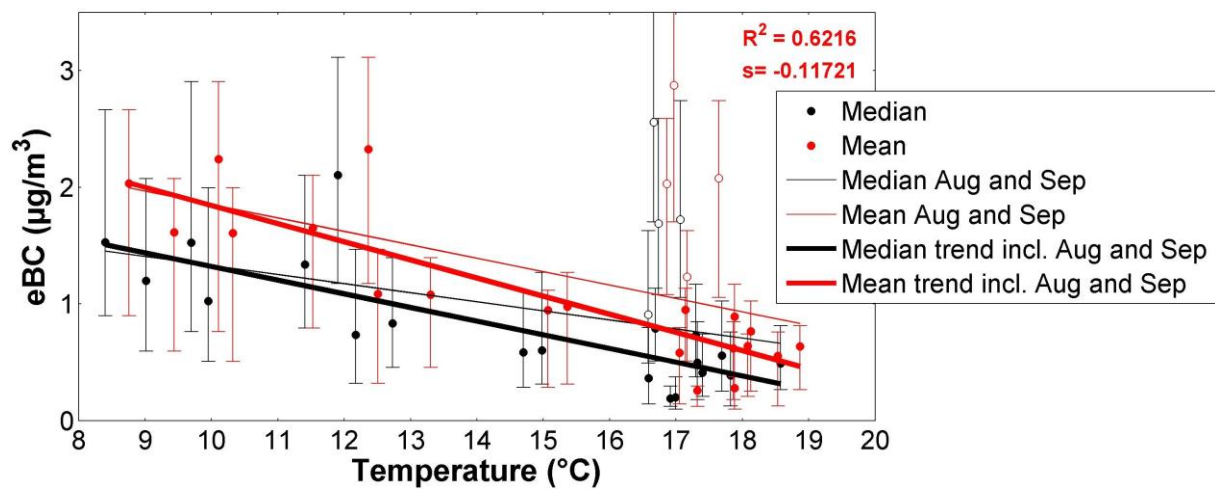


Figure 11. Monthly median and mean eBC (with bars indicating 25<sup>th</sup> and 75<sup>th</sup> percentiles) plotted against monthly median and mean temperatures for Elandsfontein.



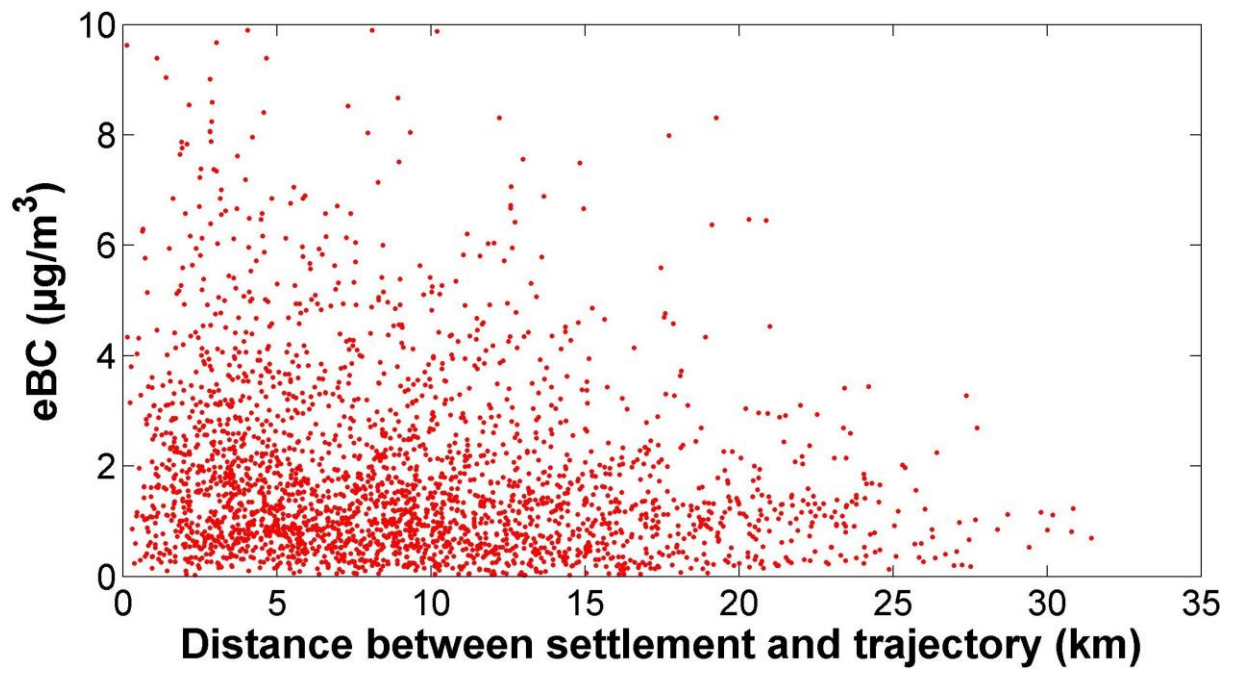
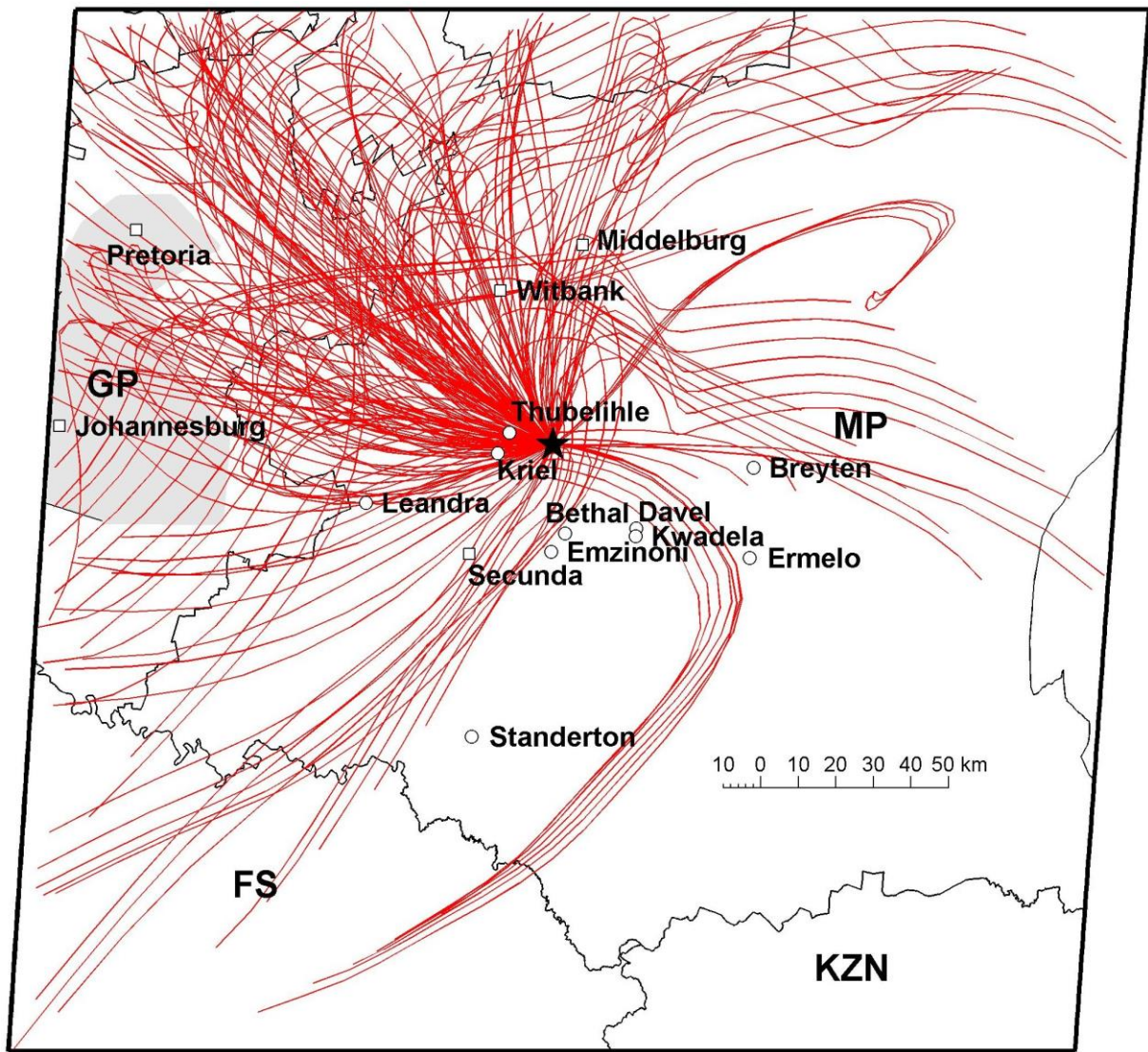
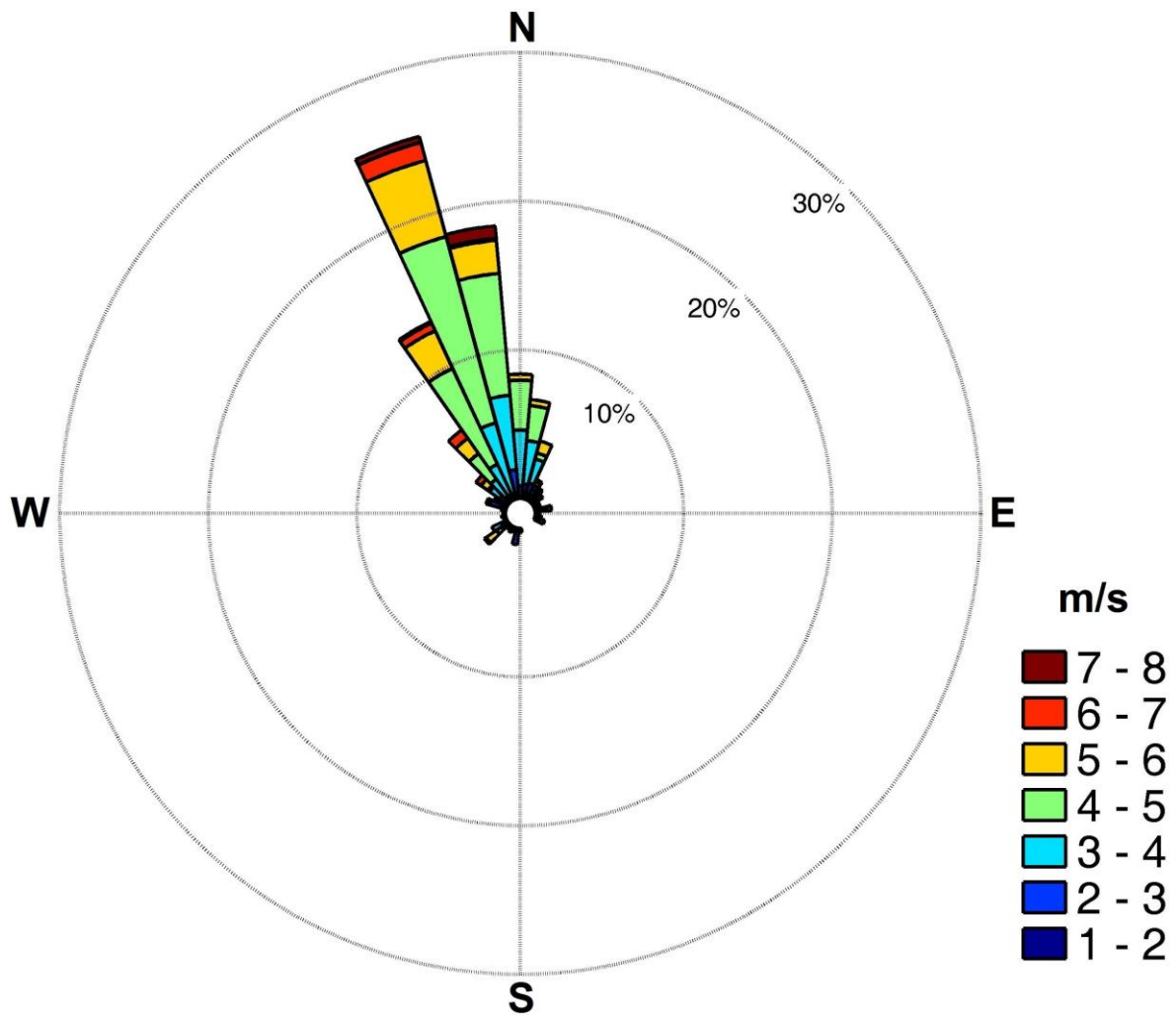


Figure 12. eBC concentration plotted against the shortest distances that hourly arriving back trajectories passed in- or semi-formal settlements during the winter months of June and July at Elandsfontein.



(a)

Figure 13. (a) Map indicating 24-hour back trajectories associated with peaks characterised by coincidental increases in eBC with  $\text{NO}_2$ ,  $\text{SO}_2$  and  $\text{H}_2\text{S}$ , but not  $\text{NO}$  in June and July. The Elandsfontein site is indicated by the black star. (b) The wind rose associated with arrival times of plumes associated with household combustion is indicated in Figure (b).



(b)

Figure 13 (continue). (a) Map indicating 24-hour back trajectories associated with peaks characterised by coincidental increases in eBC with  $\text{NO}_2$ ,  $\text{SO}_2$  and  $\text{H}_2\text{S}$ , but not with  $\text{NO}$  in June and July. The Elandsfontein site is indicated by the black star. (b) The wind rose associated with arrival times of plumes associated with household combustion is indicated in Figure (b).

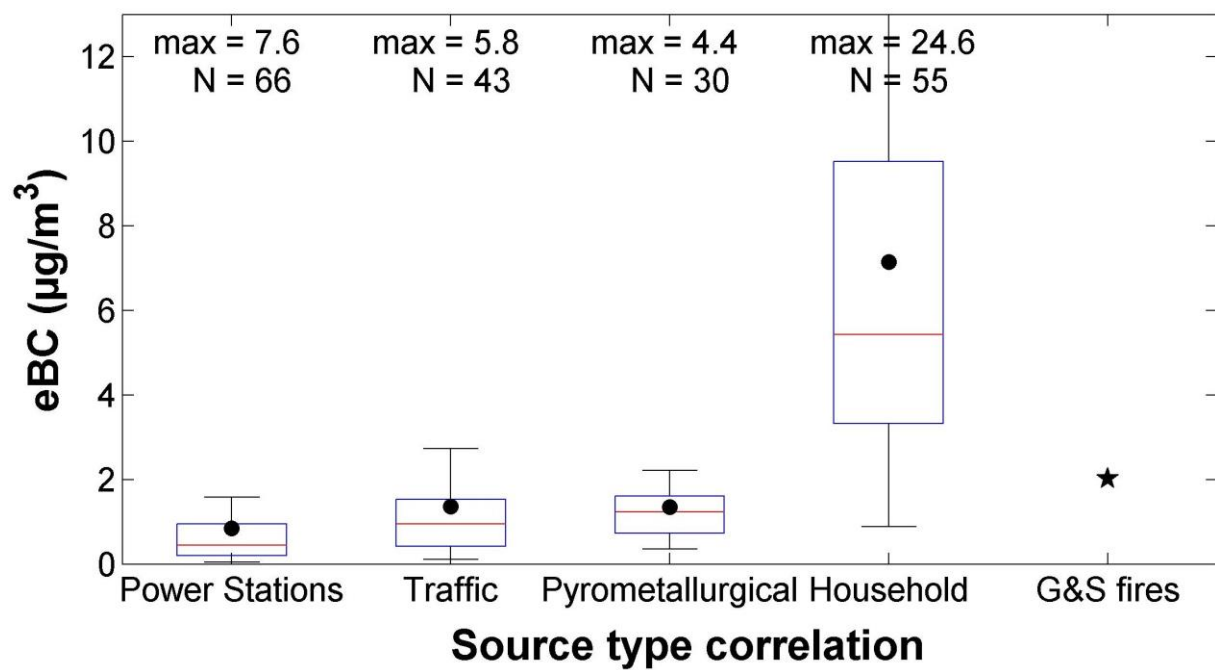


Figure 14.  $\Delta$  eBC measured during plumes when eBC increases originated from coal-fired power station, traffic, pyro-metallurgical smelters and household combustion as measured at Elandsfontein. The overall mean baseline increase due to savannah and grassland fires (G&S fires) in September is also indicated. This data was normalised to variations in boundary layer at Elandsfontein (Korhonen et al., 2014).

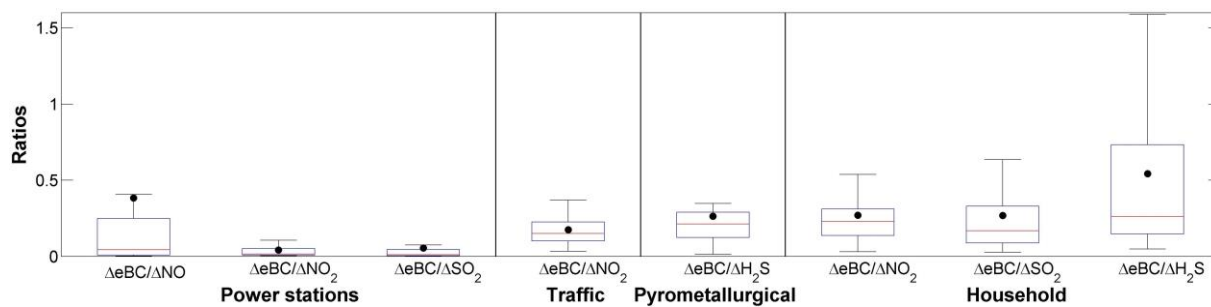


Figure 15. Ratio of  $\Delta eBC$  divided by  $\Delta$  of other species relevant to the identification of each source type, except for grassland and savannah fires measured at Elandsfontein.

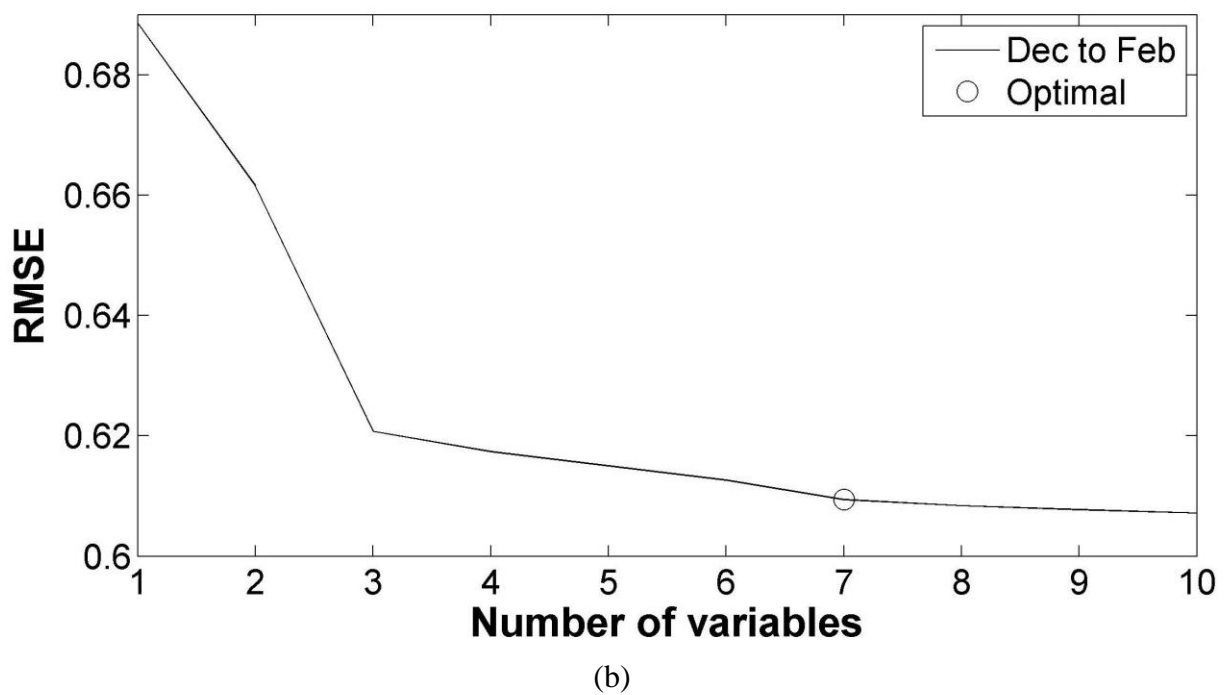
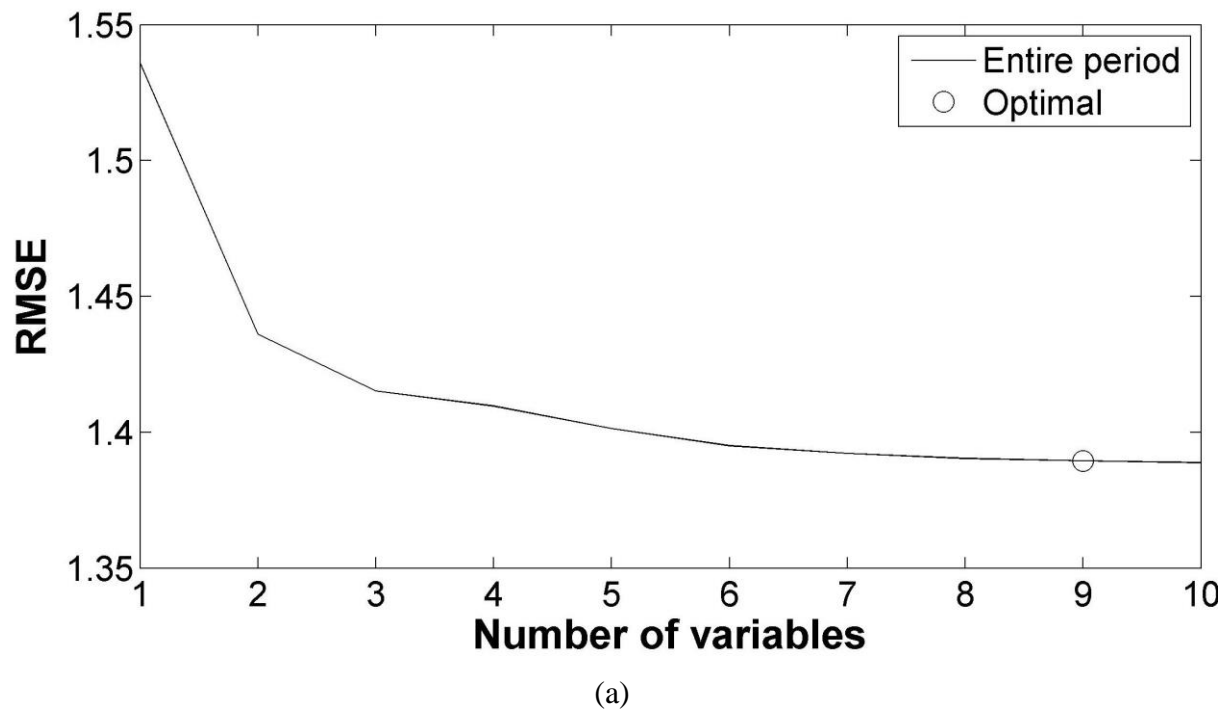
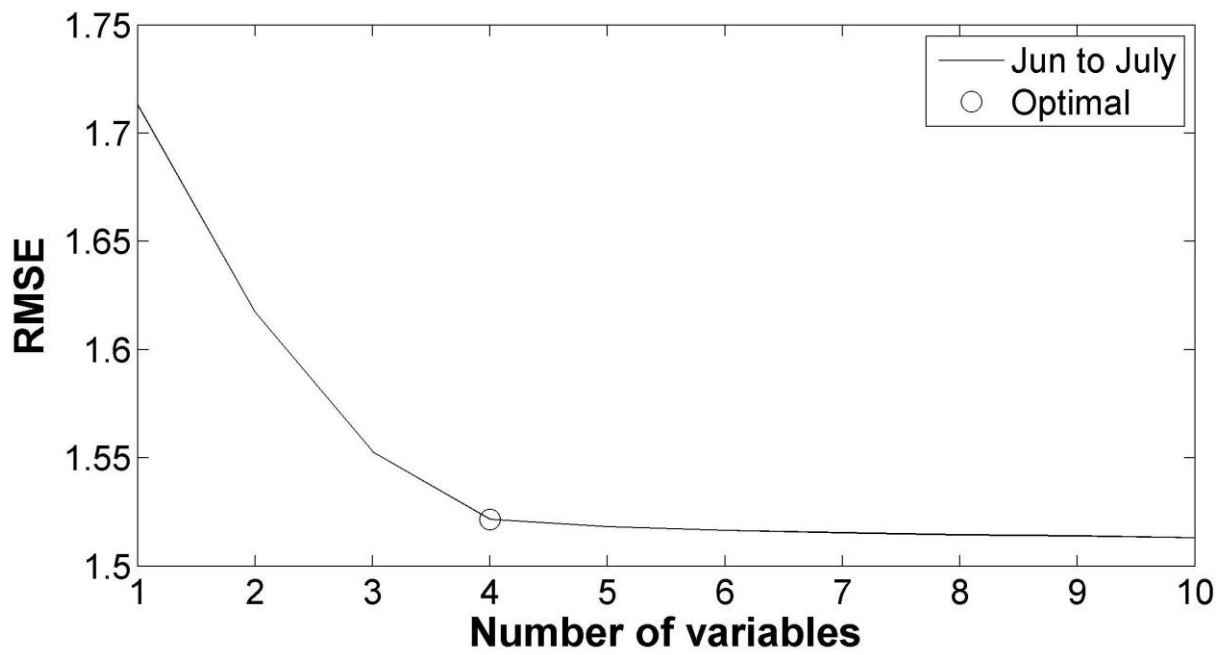
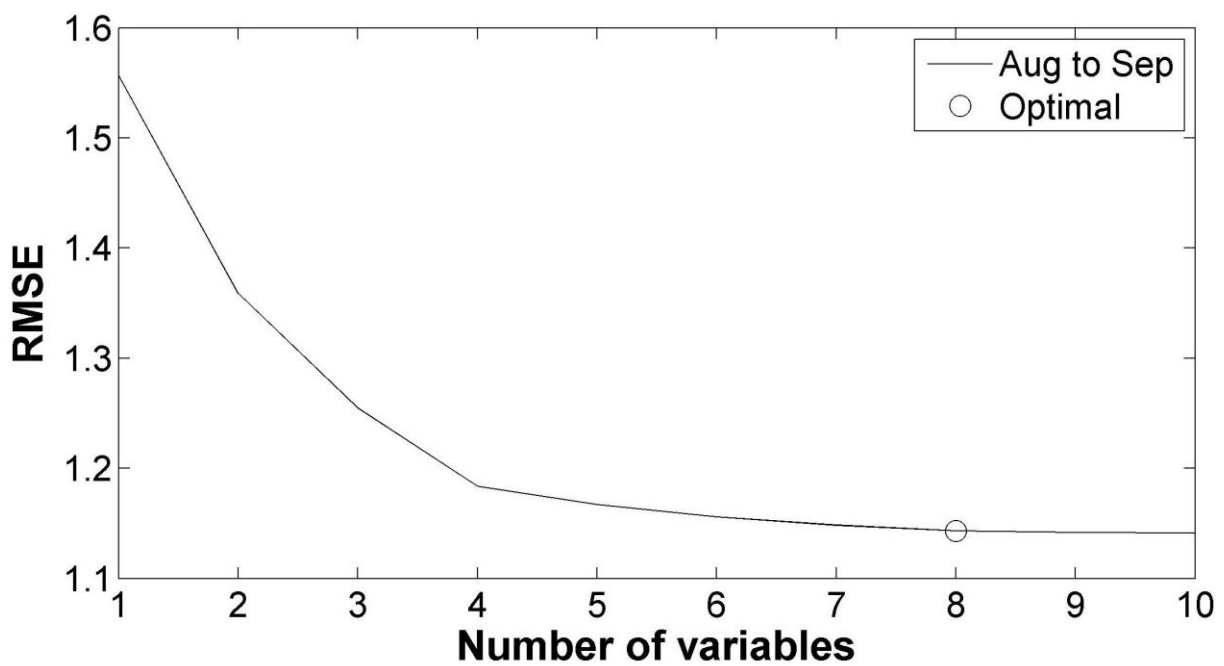


Figure 16. RMSE difference between the MLR calculated eBC and the actual measured eBC at Elandsfontein for the entire measurement period (a), as well as the December to February (b), June to July (c) and August to September (d) periods individually.



(c)



(d)

Figure 16 (continue). RMSE difference between the MLR calculated eBC and the actual measured eBC at Elandsfontein for the entire measurement period (a), as well as the December to February (b), June to July (c) and August to September (d) periods individually.

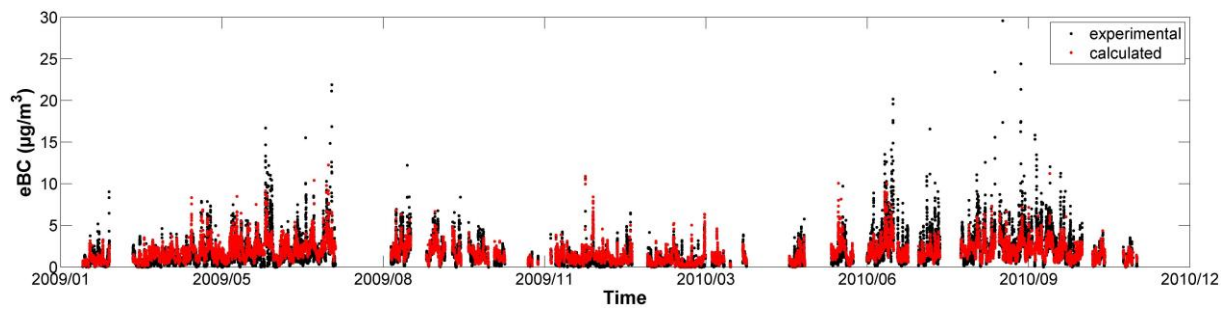


Figure 17. Actual eBC compared with calculated (using Eq. 2) for the entire monitoring period at Elandsfontein.